



**QUEEN'S
UNIVERSITY
BELFAST**

Mechanochemical Synthesis of Pharmaceutical Cocrystal Suspensions via Hot Melt Extrusion: Feasibility Studies and Physicochemical Characterisation

Li, S., Yu, T., Tian, Y., McCoy, C. P., Jones, D. S., & Andrews, G. P. (2016). Mechanochemical Synthesis of Pharmaceutical Cocrystal Suspensions via Hot Melt Extrusion: Feasibility Studies and Physicochemical Characterisation. *Molecular Pharmaceutics*, 13(9), 3054–3068.
<https://doi.org/10.1021/acs.molpharmaceut.6b00134>

Published in:
Molecular Pharmaceutics

Document Version:
Peer reviewed version

Queen's University Belfast - Research Portal:
[Link to publication record in Queen's University Belfast Research Portal](#)

Publisher rights
Copyright 2016 American Chemical Society.

General rights
Copyright for the publications made accessible via the Queen's University Belfast Research Portal is retained by the author(s) and / or other copyright owners and it is a condition of accessing these publications that users recognise and abide by the legal requirements associated with these rights.

Take down policy
The Research Portal is Queen's institutional repository that provides access to Queen's research output. Every effort has been made to ensure that content in the Research Portal does not infringe any person's rights, or applicable UK laws. If you discover content in the Research Portal that you believe breaches copyright or violates any law, please contact openaccess@qub.ac.uk.

Open Access
This research has been made openly available by Queen's academics and its Open Research team. We would love to hear how access to this research benefits you. – Share your feedback with us: <http://go.qub.ac.uk/oa-feedback>

1 **Mechanochemical Synthesis of Pharmaceutical Cocrystal Suspensions via Hot Melt**
2 **Extrusion: Feasibility Studies and Physicochemical Characterisation**

3

4 **Shu Li, Tao Yu, Yiwei Tian, Colin P. McCoy, David S. Jones and Gavin P. Andrews***,

5 Pharmaceutical Engineering Group, School of Pharmacy, Medical Biology Centre,

6 Queen's University, Belfast BT9, Northern Ireland

7

8

9 **Correspondence to:* Gavin P. Andrews (Telephone: +44-2890-97-2646; E-mail:

10 g.andrews@qub.ac.uk)

11

12

13

14 **Running Title:** Cocrystals via Mechanochemistry

15

16 **Abstract:**

17 Engineered Cocrystals offer an alternative solid drug form with tailored
18 physicochemical properties. Interestingly, although cocrystals provide many
19 new possibilities they also present new challenges, particularly in regard to their
20 design and large-scale manufacture. Current literature has primarily focused on
21 the preparation and characterization of novel cocrystals typically containing only
22 the drug and coformer, leaving the subsequent formulation less explored. In this
23 paper we propose, for the first time, the use of hot melt extrusion for the
24 mechanochemical synthesis of pharmaceutical cocrystals in the presence of a
25 meltable binder. In this approach, we examine excipients that are amenable to
26 hot melt extrusion, forming a suspension of cocrystal particulates embedded in a
27 pharmaceutical matrix. Using ibuprofen and isonicotinamide as a model
28 cocrystal reagent pair, formulations extruded with a small molecular matrix
29 carrier (xylitol) were examined to be intimate mixtures wherein the newly
30 formed cocrystal particulates were physically suspended in a matrix. With
31 respect to formulations extruded using polymeric carriers (Soluplus® and
32 Eudragit® EPO, respectively), however, there was no evidence within PXRD
33 patterns of either crystalline ibuprofen or the cocrystal. Importantly, it was
34 established in this study that an appropriate carrier for a cocrystal reagent pair
35 during HME processing should satisfy certain criteria including limited
36 interaction with parent reagents and cocrystal product, processing temperature
37 sufficiently lower than the onset of cocrystal T_m , low melt viscosity and rapid
38 solidification upon cooling.

39 **Introduction**

40 Pharmaceutical material science is fundamental in the design and development
41 of new and improved drug delivery platforms. In particular, crystal engineering
42 has brought the possibility of designing new drug complexes (cocrystals) that
43 provide an opportunity to modify the properties of the parent drug. Possible
44 improvements include solid-state properties, aqueous solubility, dissolution rate
45 and bioavailability¹⁻³, the latter being particularly important for BCS Class II
46 drugs. Undoubtedly, over the last decade, the use of crystal engineering to
47 optimise the physical properties of drugs has gained significant attention^{4,5}. This
48 may be attributed to the fact that the effective delivery of drugs to a patient in a
49 safe and cost-effective manner is significantly influenced by the physicochemical
50 properties of drug in the solid state. Moreover, cocrystals manufactured via
51 crystal engineering offer an alternative solid drug form with tailored
52 physicochemical properties and represent a significant opportunity to generate
53 intellectual property. Interestingly, although cocrystals provide many new
54 possibilities they also present new challenges, particularly in regard to their
55 design and large-scale manufacture.

56 Pharmaceutical cocrystals are multi-component molecular complexes
57 consisting of a drug and a cocrystal former (coformer) in a well-defined
58 stoichiometry, formed mainly via hydrogen bonding, halogen bonds and/or π - π
59 stacking supramolecular interactions⁴⁻⁶. The wide range of coformer properties
60 and interactions in solid and solution phase (depending upon manufacturing
61 method) provides an opportunity to alter physicochemical properties. It has
62 been previously reported that successful cocrystallization requires
63 complimentary functional groups on drug and coformer, typical examples
64 including carboxylic acids and amides⁷.

65 Cocrystals are traditionally manufactured using traditional solvent
66 evaporation^{8,9}. However, more recently there has been a strong and increasing
67 demand for clean and environmentally friendly processes that focus on green
68 methods of conducting chemical reactions in the absence of solvents. Of
69 particular relevance within the pharmaceutical arena has been the recent
70 interest in, and success of, grinding methods, for pharmaceutical
71 cocrystallisation via mechanochemical reactions¹⁰⁻¹³. This has been driven by the

72 fact that pharmaceutical cocrystal synthesis is largely due to the formation of
73 supramolecular interactions that can be broken and reformed under mild
74 mechanical conditions.

75 Dry/neat grinding, are simple and commonly used processes for
76 mechanochemical synthesis within solid blends¹⁴. These techniques have
77 emerged as a useful, alternative technique to the traditional solvent-intensive
78 methods for pharmaceutical cocrystal synthesis and production. However, there
79 has been a number of reports presenting incomplete cocrystallisation using dry
80 grinding¹⁵. Liquid-assisted grinding has, therefore, gained considerable favour
81 because of the possibility of providing dramatically improved productivity via
82 the addition of only small amounts of liquid to a typical grinding process¹⁶⁻²⁴. It
83 is, however, occasionally criticised for the unintentional production of cocrystal
84 solvates²⁵. In addition, the role of the added liquid differs from case to case,
85 resulting in difficulties in clarifying reaction mechanisms^{16,20,26}. More recently,
86 another advanced solvent-free continuous manufacturing method, hot-melt
87 extrusion (HME), has also emerged as an, easy to scale, alternative for
88 mechanochemical cocrystal synthesis²⁷⁻³¹. Interestingly, current literature has
89 primarily focused on the preparation and characterization of novel cocrystals
90 typically containing only the drug and coformer, leaving the subsequent
91 formulation less explored³². IN this regard, Etter *et al* (1993) reported
92 cocrystallisation in the presence of a third component by solid-state grinding³³.
93 The resulting product contained cocrystals of the complementary reagent pair,
94 as well as the additional inert component that remained unchanged following
95 cocrystal manufacture. Furthermore, cocrystals formed in the presence of the
96 inert component had the same crystal structure as cocrystals grown from
97 solution. More recently, driven by polymer-induced heteronucleation studies³⁴, it
98 has also been shown that the involvement of macromolecules in the cocrystal
99 pool may also catalyse the reaction during mechanochemical preparation of
100 cocrystals³⁵. The cocrystals manufactured using polymer-assisted grinding
101 methods were shown to negate the risk of generating undesirable solvates, while
102 providing excellent control over the particle size of the resultant cocrsytals.
103 Moreover, other important work has investigated cocrystal manufacture in the
104 presence of an inert excipient³⁶. The effects of cofomers on phase

105 transformation and release profiles of carbamazepine (CBZ) cocrystals in
106 hydroxypropyl methylcellulose (HPMC) matrix tablets were examined. It was
107 shown that HPMC partially inhibited the crystallisation of CBZ during dissolution.

108 If mechanochemical synthesis is to deliver its promise of being a clean
109 manufacturing technology, it must be shown to be capable of operating in an
110 environment devoid of solvent and be scalable. Furthermore, it is well
111 recognised that cocrystal synthesis is only one step in the development of
112 suitable oral dose formulations with other components (e.g., lubricant, glidant,
113 diluent) and unit operations (milling, sieving, blending, compression, filling)
114 being required before a successful drug product is produced. In light of the
115 above, we propose, for the first time, the use of hot melt extrusion, a solventless,
116 continuous and easily scalable technique, for the mechanochemical synthesis of
117 pharmaceutical cocrystals in the presence of a meltable binder. In this approach,
118 we examine chemically inert excipients that are amenable to hot melt extrusion,
119 forming a suspension of cocrystal particulates embedded in a pharmaceutical
120 matrix. We aim to understand if inert meltable carriers can be used to facilitate
121 the production of a solid extrudate while also acting as a catalyst for
122 cocrystallisation during melt-extrusion processing.

123

124 **Selection of Formulation Components**

125 ***Cocrystal Reagents***

126 Ibuprofen (Ibu, Figure 1a) is a BCS Class II drug³⁷ and has dissolution limited
127 absorption, particularly in acidic environment. Ibu has been widely used as a
128 cocrystal reagent, principally because it is inexpensive and contains a carboxylic
129 acid functional group that makes it an excellent donor to form intermolecular
130 hydrogen bonds with cocrystal reagents that possess a lone pair of electrons³⁸.

131 Isonicotinamide (IsoNA, Figure 1a), although not classified as a GRAS
132 substance, has been shown to be an effective cofomer with many literature
133 examples of carboxylic acid-IsoNA cocrystals³⁹⁻⁴¹.

134

135 ***Matrix Excipients***

136 Recently it has been demonstrated that a small molecular weight sugar alcohol,
137 mannitol, could be used as a matrix platform capable of significantly increasing

138 the dissolution rate of poorly water soluble drugs⁴². In the work reported by
139 Thommes et al., (2011) HME was used to manufacture a suspension of
140 crystalline drug in a molten excipient to produce a uniform distribution of fine
141 particles. Rapid crystallization of mannitol 'fixed' the suspended drug particles
142 producing a solid homogeneous extrudate. In the work described in this article,
143 we adapt the concept of extruded crystalline suspensions and apply the
144 aforementioned preliminary criteria into matrix carrier selection. However, due
145 to thermal stability considerations, mannitol, which melts at 160°C, was not used.
146 Consequently, xylitol which melts at a significantly lower temperature was
147 employed.

148 Despite the advantages sugar alcohols offer with respect to low melt viscosity
149 and rapid solidification, extrudates may be difficult to shape post extrusion
150 owing to the rigidity of their crystalline structure. Thus, the use of thermoplastic
151 polymers was also examined. Eudragit® E PO and Soluplus® were chosen for
152 such purposes owing to their relatively low T_g and hence wider processing
153 window. If cocrystals can be successfully manufactured and precipitated from an
154 amorphous polymeric carrier, an amorphous suspension also referred to as a
155 glass suspension could be formulated.

156

157 **Materials & Methodology**

158 ***Materials***

159 Ibuprofen, isonicotinamide, and xylitol were purchased from Sigma-Aldrich (St.
160 Louis, MO, USA). Eudragit®E PO was obtained from Evonik (Essen, Germany).
161 Soluplus® was kindly supplied by BASF Corporation (Ludwigshafen, Germany).
162 All other chemical reagents used were of analytical grade.

163

164 ***Differential Scanning Calorimetry (DSC)***

165 Cocrystallisation feasibility studies and extrudate analyses were conducted on a
166 DSC 4000 (heat flux single furnace), and a DSC 8000 (power compensation dual
167 furnace), respectively (Perkin-Elmer, Windsor, Berkshire, UK). Both instruments
168 were calibrated at the respective ramp rates with indium and zinc for both
169 melting point and heat of fusion. Either dry nitrogen or helium was purged at a
170 flow rate of 40mL/min through the sample and reference cells to maintain an

171 inert atmosphere. 3-5mg of sample was accurately weighed into an aluminium
172 pan and crimped using an aluminium pan lid. The crimped pan set was then
173 subjected to a thermal ramp at 20°C/min in DSC 4000, and 200°C/min in DSC
174 8000, respectively, from -60°C to 200°C. The polymeric candidates were
175 subjected to modulated DSC (TA Q100, TA Instruments) at 2°C/min, with an
176 amplitude and frequency of $\pm 0.6^\circ\text{C}$ every 40s to enable the determination of the
177 glass transition temperature (T_g).

178

179 ***Thermogravimetric Analysis (TGA)***

180 The decomposition temperature for each individual substance was determined
181 using a Thermal Advantage Model Q500 TGA (TA instruments, Leatherhead, UK).
182 Ramp tests were performed on powdered samples (5-10 mg) heated at
183 10°C/min over a range from 0°C to 400°C. Dry nitrogen (flow rate sample: 60
184 mL/min, flow rate balance: 40 mL/min) was purged through the sample
185 chamber during all experiments to maintain an inert environment and hence
186 prevent oxidation. The temperature at which a 5% weight loss occurred was
187 recorded for each sample and considered as the onset of material decomposition.

188

189 ***Preparation of the Reference Cocrystal Standard***

190 0.01 moles of equimolar ibuprofen-isonicotinamide mixture was dissolved in
191 50mL methanol and stirred at room temperature until complete dissolution was
192 achieved. The resulting clear solution was left in a fume hood covered with a
193 funnel to allow slow evaporation of the solvent for 48 hours. The precipitate was
194 collected and subsequently stored in an oven at 45°C for a further 24 hours to
195 remove any residual solvent. The resulting material was gently pulverized using
196 a mortar and pestle, sized through a 220 μm sieve and stored in a vacuum
197 desiccator before being subjected to further analysis.

198

199 ***Cocrystallisation via Ball-Milling***

200 Equimolar ibuprofen-isonicotinamide mixtures with or devoid of excipient were
201 ground using a ball mill (MM200, Retsch, Reinische, Haan, Germany) at a
202 frequency of 20 s⁻¹ frequency for pre-determined periods of time (i.e. 2, 5, 8, 15,

203 30, 45 and 60 minutes). The resulting pulverized mixtures were sized through a
204 220 μ m sieve before being subjected to further characterisation.

205

206 ***Cocrystallisation via Hot-Melt Extrusion***

207 Physically mixed blends of each formulation were manually fed into a co-rotating
208 twin-screw HAAKE Mini-lab Extruder (HAAKE Minilab, Thermo Electron
209 Corporation, Stone, Staffordshire, UK). The process temperature was determined
210 according to the melting temperature(s) of the crystalline compound(s) in the
211 physical blend with screw speed set at 10rpm. For the formulations containing
212 xylitol, the HME parameters were slightly modified to prevent early-stage phase
213 separation and late-stage die blockage. In particular, the processing was divided
214 into two stages: the 'feeding stage' where temperature was set at the melting
215 point of the polyol and screw speed set at 10rpm; and the 'flushing stage' where
216 temperature was set 7°C lower than the polyol melting temperature and screw
217 speed set at 50rpm (Table 1). All collected products were pulverized by mortar
218 and pestle and subsequently stored in a desiccator over silica gel at room
219 temperature prior to further analyses.

220

221 ***Powder X-ray Diffraction (PXRD)***

222 Samples were analysed at room temperature using a MiniFlex II Desktop Powder
223 X-ray Diffractometer (Rigaku Corporation, Kent, England) equipped with Cu K β
224 radiation, at a voltage of 30 kV and a current of 15 mA. The powdered samples
225 were gently consolidated on a glass top-loading sample holder with 0.2mm
226 depression. All samples were scanned within the angular range of 1.5-40° 2 θ in
227 continuous mode with a sampling width of 0.03° and a scan speed of 2.0°/min.

228

229 ***Quantification of Cocrystal Yielding***

230 The peak area of the cocrystal characteristic peak at 3.3° 2 θ for each sample was
231 used to determine the cocrystal yield⁴³. A series of physical mixtures containing
232 the reference cocrystal and xylitol at 10 different cocrystal loadings, 10, 20, 30,
233 40, 50, 60, 70, 80, 90 & 100% w/w, respectively, were prepared through gentle
234 mixing. The blended samples were placed into a 0.2mm-deep squared
235 indentation on the glass sample holder for PXRD analysis. The integration region

236 was set between [2.400~4.050° 2θ] with manual background subtraction using
237 the IntegralAnalysis Version 6.0 (Rigaku Corporation, Kent, England). A
238 calibration curve, $y=284.877x-668.959$ ($R^2=0.998$) was constructed using linear
239 regression of the average peak area against theoretical cocrystal concentration
240 in the blends. The calibration curve was validated for linearity, accuracy,
241 precision, LoD and LoQ according to the methods recommended in the ICH
242 guidelines⁴⁴ (data included as supporting documents).

243

244 ***FT Infrared Spectroscopy (FTIR)***

245 FT-IR spectroscopy was used to investigate molecular interactions and to
246 identify the structure of Ibu/IsoNA cocrystal. Experiments were performed using
247 a Fourier transform infrared spectrophotometer model 4100 (FT/IR-4100)
248 (Jasco, Easton, MD), incorporated with the Version 2 Jasco Spectra Manager
249 Software. A scanning range of 4000-400 cm^{-1} with 4.0 cm^{-1} resolution and 16
250 scans per spectrum was used for all samples. Prior to FTIR spectroscopic
251 analysis, samples were gently ground with dry potassium bromide (KBr) powder
252 using an agate mortar and pestle and compressed at approximately 7.5Pa for 60s
253 to prepare a KBr disk. The concentration of the samples in a KBr disk was
254 maintained at 0.67% (2mg sample plus 298mg KBr) for all analyses.

255

256 ***Raman Microscopy & Mapping***

257 Raman spectroscopic analyses were conducted using a RamanMicro 300 Raman
258 microscope (Perkin Elmer, Windsor, Berkshire, UK) coupled with an Avalon
259 Raman station R3 Model AVRS003A spectrometer (Avalon Instruments, Belfast,
260 UK). A magnification of 20x with a total exposure time of 20s (4s acquisition \times 5)
261 was used for all samples. Data was collected from 200-3200 cm^{-1} and analysed
262 using Spectrum v6.3.4 software with an automatic baseline correction. Cross
263 sections of rod shaped extrudates were mapped with a 50 μm spacing between
264 each sampling point. Approximately 4000 points were collected across the
265 exposed mapping area for the cross section of one pellet. The laser power was
266 set at 80% throughout the mapping process to avoid sample saturation.
267 Spectrum IMAGE R1.6.4.0394 software was used to conduct mapping analysis
268 for each examined sample. The characteristic peak associated with the

269 Ibu/IsoNA cocrystal at 1020 cm⁻¹ was used in the single wavenumber mode. The
270 maps were shown with an ordinate axis range of [1000-7500 INT], whilst the
271 horizontal X axis range and the vertical Y axis range were both 0-2350 μm. A
272 rainbow cubic look-up table was utilized to illustrate the intensity of the chosen
273 cocrystal peak.

274

275 ***Polarized Light Microscope (PLM)***

276 A polarized light microscope (Olympus BX50F4, Microscope Service and Sales,
277 Surrey, UK) was used to study the morphology of the melt-extruded cocrystals in
278 comparison to that of the unprocessed ibuprofen. Polarized light micrographs of
279 each sample were captured at room temperature using a Pixelink Megapixel
280 Firewire Camera and Pixelink software (Scorpion Vision Ltd., Lymington, UK).
281 The milled sample within the size range 180~212μm was dispersed in a drop of
282 mineral oil on a glass slide. All measurements were performed at a magnification
283 of 200x with the polariser and analyser positioned perpendicularly.

284

285 ***In-vitro Dissolution Study***

286 In-vitro drug dissolution tests were conducted to evaluate solubility
287 enhancement and dissolution behaviour of the melt extruded Ibu/IsoNA
288 cocrystals in comparison with that of the unprocessed ibuprofen. Release studies
289 were performed using a Caleva dissolution tester 10ST (GB Caleva Ltd., Dorset,
290 UK) according to the BP 2011 apparatus II, paddle method. The powdered
291 samples were sieved to the same particle size [180~212μm] prior to testing.
292 Each formulation, containing equivalent to 120mg Ibu, was tested in 600mL
293 deionized water at 37±0.5°C using a paddle rotation speed of 75rpm. 3mL
294 aliquots were withdrawn from each dissolution vessel at regular time intervals
295 and filtered through a 0.45μm Millipore filter unit (MILLEX®-GS, Millipore,
296 Carrigtwohill Co, Cork, Ireland) before being subjected to a validated HPLC
297 analysis. Immediately after sample withdrawal, 3mL of blank dissolution media
298 was added into each vessel to maintain the overall media volume.

299

300 **High Performance Liquid Chromatography (HPLC)**

301 The concentration of ibuprofen in each sampled aliquot was determined using
302 HPLC analysis. The HPLC system consisted of a Waters binary HPLC pump 1525,
303 a Plus Auto sampler 717, an In-line Degasser AF and a Dual λ Absorbance
304 Detector 2487 (Waters, Massachusetts, USA). Sampled aliquots were analysed at
305 220 nm using a Jupiter C18 300 column (5 μ m) with a length of 250 mm and a
306 diameter of 4.60 mm (Phenomenex, Macclesfield, UK). The mobile phase
307 consisted of 85% methanol and 15% deionized water containing 0.2% TFA. The
308 flow rate was set at 1 mL/min and the column chamber was maintained at 40°C
309 for the entire analytical procedure. The average retention times under these
310 conditions were 4.56 minutes for Ibu, 3.40 minutes for IsoNA, while other
311 components were tested to show no interference. When Soluplus® was involved,
312 the mobile phase was changed to a 70:30 ratio between the organic and
313 inorganic solutions with a retention time of 8.76 minutes for ibuprofen to avoid
314 interference. Peak areas were calculated using Breeze 3.30 software. Standard
315 solutions were prepared in triplicate using methanol and deionized water at 1:1
316 volume ratio for the generation of a linear calibration curve ($R^2 > 0.999$). The
317 calculated concentrations of ibuprofen dissolved during the dissolution test were
318 then plotted as a function of time.

319

320 **Storage Stability**

321 The extruded suspensions were stored either in a desiccator over silica gel for 12
322 months under ambient conditions or in a desiccator over saturated sodium
323 chloride solution at 20°C and 70%RH for 12 months. The aged suspensions were
324 examined by PXRD and the cocrystal content in each formulation was calculated
325 using the aforementioned yielding quantification.

326

327 **Statistical Analysis**

328 Statistical analyses were conducted using a one-way analysis of variance
329 (GraphPad Prism 6.0). Individual differences between treatment groups were
330 identified using Tukey's *post-hoc* test with $P < 0.05$ denoting statistical
331 significance.

332

333 Results

334 *Formation of Ibu/IsoNA Cocrystal*

335 In this work we considered that Ibu and IsoNA would form a cocrystal at an
336 equimolar stoichiometric ratio⁴⁵⁻⁴⁸. This would be facilitated by the interaction
337 of the carboxylic acid functional group of Ibu, the IsoNA amide and the N on the
338 pyridine of IsoNA²⁶. With respect to IBu and IsoNA, the carboxylic acid group,
339 would be highly pertinent in successful formation of cocrystal with carboxylic
340 acid-aromatic nitrogen and carboxylic acid-amide synthons being the major
341 interactions present (Figure 1b).

342 Prior to addition of pharmaceutical excipients and evaluation of extrusion as a
343 continuous process for mechanochemical synthesis of cocrystals, we employed
344 ball milling to determine the feasibility of forming a cocrystal product from an
345 Ibu/IsoNA blend at a 1:1 molar ratio. Conventional DSC analysis at a heating rate
346 of 20°C/min was used to confirm the formation of the Ibu/IsoNA cocrystal. It has
347 been previously reported in many articles that the melting temperature (T_m) of
348 cocrystal is often between that of the drug and the coformer, or lower than both
349 individual T_m values. The DSC thermograms for Ibu, IsoNA, and their equimolar
350 physical mixtures are shown in Figure 2. Ibu and IsoNA exhibited characteristic
351 melting points, when heated using a ramp rate of 20°C/min, at approximately
352 80.58±0.32°C and 161.56±0.59°C, respectively. Physically mixed and ball-milled
353 samples exhibited DSC traces devoid of an endothermic peak characteristic of
354 IsoNA melting and importantly, a new endothermic event, considered to be the
355 heat of fusion for a cocrystal was observed at approximately 123°C. The enthalpy
356 associated with this peak increased in value as a result of increasing mechanical
357 energy (physically mixed sample (50.1±0.77 J/g); 2 minutes milling (148.6±0.83
358 J/g); 5 minutes milling (155.6±1.02 J/g)). Moreover, ball milled samples
359 exhibited an Ibu melting peak that was significantly depressed, decreasing from
360 80.58±0.32°C to 73.97±0.56°C and 72.03±0.04°C for 2 minutes and 5 minutes
361 milling, respectively. The enthalpy of these two transitions was also significantly
362 lowered. Moreover, there was no evidence of a melting endotherm for crystalline
363 IsoNA in the DSC thermograms where Ibu was present. From the data, it would
364 appear that once Ibu melted, IsoNA dissolved in the molten drug.

365 The addition of 10% xylitol, as shown in Figure 3, considerably decreased the

366 value of enthalpy associated with the cocrystal peak from 148.6 ± 0.83 J/g to
367 62.46 ± 0.64 J/g after 2 minutes milling. In this case it is important to note that the
368 maximum enthalpy expected for the formulations incorporating 10% w/w
369 xylitol would be approximately 133 J/g (0.9×148.6). The enthalpy observed at 2
370 minutes milling in the presence of 10% Xylitol was approximately 48% of what
371 was expected. The enthalpy, nonetheless, increased significantly with increasing
372 duration of milling, reaching 124.69 ± 1.13 J/g (96% of value observed for neat
373 cocrystallisation) after 45 minutes of consecutive milling. A further 15 minutes
374 milling processing, however, decreased the measured cocrystal ΔH to
375 107.25 ± 0.98 J/g. In all cases, there was a clear melting endotherm present for
376 Xylitol suggesting that, unlike IsoNA, it remained crystalline following Ibu
377 melting.

378

379 **Hot Melt Extrusion**

380 Hot melt extrusion is a non-ambient process that forces materials through a
381 heated barrel. Processing parameters and formulation variables have a
382 significant impact upon the properties of extruded product. The process
383 parameters and associated observations made during HME are listed in Table 1.
384 The incorporation of polymeric matrix carriers (formulations 2 and 3)
385 significantly reduced the torque values, when compared with formulation 1 (Net
386 cocrystal reagents). The addition of 10% w/w xylitol resulted in an increase of
387 torque from 40-44Ncm up to 109-122Ncm and a reduction in the residence time
388 from 233s to 90s. A further increase in the xylitol concentration to 30% w/w
389 decreased the torque to 43-59Ncm, similar to the torque values recorded for
390 formulation 1. A further increase in the concentration of xylitol to 50% w/w
391 reduced the torque to 19-22Ncm. Interestingly, decreasing torque values
392 progressing through formulations 4, 5 and 6 resulted in residence times that
393 were increased. The addition of xylitol (30% and 50%) increased residence time
394 to 272s and 329s, respectively.

395

396 **Thermal Analysis**

397 When using conventional DSC at a heating rate of $20^\circ\text{C}/\text{min}$ during preliminary
398 study, physically mixed Ibu and IsoNA blends showed only endothermic events

399 typical of the melting of Ibu and the Ibu/IsoNA cocrystal (Figure 2). By using
400 hyper DSC (200°C/min), however, it was possible to observe an endothermic
401 peak characteristic of the melting of the residual IsoNA content. The
402 thermograms provided by hyper DSC measurements for pure Ibu, IsoNA, xylitol
403 and their extruded mixtures are presented in Figure 4. Ibu and IsoNA exhibited
404 characteristic melting points (peak) at $84.41 \pm 0.57^\circ\text{C}$ and $163.26 \pm 0.99^\circ\text{C}$,
405 respectively, when heated using a ramp rate of 200°C/min. The DSC trace
406 obtained for the reference cocrystal, precipitated from solution, showed one
407 single endothermic event, typical of a melting transition ranging from
408 $120.78 \pm 0.03^\circ\text{C}$ to $134.59 \pm 0.43^\circ\text{C}$, with the peak maximum at $127.29 \pm 0.55^\circ\text{C}$.

409 At such relatively fast heating rate, xylitol melted at $104.17 \pm 0.29^\circ\text{C}$ and
410 displayed a broad melting peak ranging from $92.98 \pm 0.13^\circ\text{C}$ to $112.30 \pm 0.17^\circ\text{C}$.
411 The similarity of melting temperatures for xylitol and the cocrystal presented
412 difficulty in using DSC to determine presence of cocrystal. This was made more
413 difficult by the fact that the melting transition associated with the cocrystal
414 showed considerable depression if measured in the presence of xylitol (Figure 4).
415 This was particularly relevant in formulations containing high concentrations of
416 xylitol. Moreover, evidence of unreacted Ibu and IsoNA could be observed in
417 thermograms associated with suspensions of 30% and 50% xylitol. However, T_m
418 of the residue of both parent components were also noticeably depressed (both
419 onset and end point).

420 Amorphous carriers Eudragit® E PO and Soluplus® showed a T_g at
421 $43.94 \pm 0.13^\circ\text{C}$ and $66.52 \pm 0.20^\circ\text{C}$, respectively (Table 2). All carrier excipients
422 studied were thermally stable whereas ibuprofen and the reference cocrystal
423 showed onset of decomposition at $197.44 \pm 3.67^\circ\text{C}$ and $164.07 \pm 6.77^\circ\text{C}$,
424 respectively.

425

426 **PXRD**

427 PXRD patterns are depicted in Figure 5. Ibu showed distinct peaks at 6.3° ,
428 16.7° , 20.2° and 22.4° 2θ , IsoNA at 17.9° , 21.0° and 23.4° 2θ , and Xylitol at 20.0° ,
429 22.5° , 22.7° and 38.4° 2θ , respectively. For the physically mixed systems the
430 PXRD data (iv) correlated well with DSC data in that there was little evidence of
431 cocrystal formation. For the extruded formulations containing Xylitol, the

432 cocrystal product (V-X) showed distinct peaks that were distinguishable from
433 simple overlap of cocrystal reagents and xylitol. New peaks were evident at 3.3°
434 and $17.1^\circ 2\theta$. The intensity of the peaks attributable to cocrystal product varied
435 as a function of excipient type and concentration. It is evident from cocrystal
436 yield that the conversion from the parent reagents to the cocrystal was
437 $28.06\pm 1.65\%$, $33.46\pm 0.55\%$, $28.60\pm 0.61\%$ and, $28.25\pm 0.65\%$ for formulations 1,
438 4, 5 and, 6, respectively. Those formulations extruded with polymeric excipient,
439 on the other hand, showed no evidence of cocrystal formation. Interestingly,
440 these diffractograms (vi and vii) showed no characteristic peaks attributable to
441 Ibu either. This would suggest that Ibu had been rendered amorphous following
442 extrusion.

443

444 ***FTIR Spectroscopic Analysis***

445 The FTIR spectra, in the $3600\text{-}2600\text{ cm}^{-1}$ and $2000\text{-}1200\text{ cm}^{-1}$ wavenumber
446 intervals, for Ibu, IsoNA, xylitol, the cocrystal reference, and the extruded
447 suspensions containing 10%, 30% and, 50% xylitol, respectively, are
448 represented in Figure 6. The assignment of IR vibrational bands in Ibu, IsoNA
449 and the equimolar reference cocrystal obtained from solution method is listed in
450 Table 3. The FTIR spectrum for Ibu showed a number of weak peaks in the
451 wavenumber region [$3100\text{-}2900\text{ cm}^{-1}$] reflecting complex modes of vibrations
452 associated to C-H, C-H₂ and C-H₃ groups⁴⁹; and a very broad peak covering
453 almost the whole wavenumber range from $3400\sim 2800\text{ cm}^{-1}$ associated to O-H
454 stretching vibrations within a carboxylic acid dimeric structure of Ibu. A sharp
455 and intense C=O stretching band at 1721.16 cm^{-1} was also observed for Ibu due
456 to the presence of a mono carboxylic acid group⁵⁰. IsoNA, on the other hand,
457 showed characteristic IR bands at: (i) 3369.03 cm^{-1} and 3185.83 cm^{-1} ,
458 representing asymmetric and symmetric $\nu_{\text{N-H}}$ stretching vibrations, respectively,
459 for the H-bonded primary amide groups among closely packed IsoNA
460 molecules^{51,52}; (ii) 1668.12 cm^{-1} , denoting $\nu_{\text{C=O}}$ stretching of the amide carbonyl
461 group⁵³; (iii) 1622.80 cm^{-1} and 1594.84 cm^{-1} for the $\delta_{\text{N-H}}$ bending vibrations of
462 the primary amide⁵⁴; and (iv) 1551.45 cm^{-1} signifying $\nu_{\text{C=N}}$ ring stretching in the
463 heterocyclic pyridine ring structure^{54,55}.

464 As shown in Figure 1, the the cocrystal structure involves a number of groups
465 with characteristic IR vibrational bands. They are the IsoNA amide N-H
466 (stretching and bending), the ISoNA amide C=O (stretching), and the pyridine N
467 of isoNA, as well as the carboxylic acid group of IBU.

468 The amide carbonyl and the pyridine N are two competing H-bond acceptor
469 sites in IsoNA structure. The pyridine N, however, is generally considered a
470 better acceptor⁵⁶, and hence more prone to attract the amide H-atom, forming a
471 N-H•••N bond in bulk IsoNA. In forming an amide homodimer synthon during
472 cocrystallisation, the amide N-H asymmetric and symmetric stretching (3369.03
473 cm⁻¹ and 3185.83 cm⁻¹) were shifted to 3434.60 cm⁻¹ and 3173.29 cm⁻¹,
474 respectively, whilst the amide carbonyl stretching vibration band (1668.12 cm⁻¹)
475 was shifted to 1629.55 cm⁻¹. The N-H blue shift to 3434.60 cm⁻¹ indicated
476 dissociation of the existing N-H•••N bond, generating free amide N-H. The N-H
477 red shift to 3173.29 cm⁻¹, together with the carbonyl red shift to 1629.55 cm⁻¹,
478 were both attributed to the formation of N-H•••O bonds between the amide N-H
479 and amide carbonyl groups in the IsoNA homodimer.

480 The lone pair of electrons on the pyridine N, after dissociation of the original
481 N-H•••N bond in bulk IsoNA, provides a strong proton acceptor site. The absence
482 of the associated Ibu O-H stretch (broad peak in the region 3400~2800 cm⁻¹)
483 provides support for dimeric dissociation in bulk Ibu. The occurrence of an
484 additional peak at 3317.93 cm⁻¹ was attributed to the formation of a
485 supramolecular heteromeric synthon through O-H•••N hydrogen bonding
486 between the pyridine N and the Ibu O-H³⁸. Moreover, in forming the carboxylic
487 acid-pyridine H-bond, the carboxylic acid carbonyl (1721.16 cm⁻¹) was red
488 shifted to 1702.84 cm⁻¹, while a C-H stretching (796.457 cm⁻¹) from the pyridine
489 ring was also red shifted to 779.101cm⁻¹, indicating formation of a C-H•••O
490 hydrogen bond within the heteromeric synthon^{39,57}. It was also apparent that the
491 addition of xylitol as a matrix carrier did not alter interactions between two
492 parent cocrystal reagents. The IR spectra of the cocrystal/xylitol suspensions
493 were typical of the spectrum of cocrystal with xylitol superimposed (Figure 6).

494

495 ***Raman Spectroscopy and Mapping***

496 As shown in Figure 7, the unprocessed Ibu, IsoNA, and their equimolar cocrystal
497 showed three distinctive peaks within Raman shift region 1050.0~975.0 cm^{-1} .
498 Ibu exhibited a peak at 1006.13 cm^{-1} characteristic of aromatic ring C-C
499 stretching. IsoNA presented a very intense and well-defined peak at 993.97 cm^{-1}
500 attributed to the pyridine ring structure. In the equimolar cocrystal, the pyridine
501 peak was broadened and the wavenumber was shifted to 1020.50 cm^{-1} . There
502 were two shoulders characteristic of the vibration of the aromatic ring of Ibu, as
503 well as the residual pyridine ring structure from the remaining free IsoNA. The
504 matrix carrier xylitol, on the other hand, did not show any distinctive peak
505 within this Raman shift region. It is, therefore, clear that the peak at 1020.50 cm^{-1} ,
506 characteristic of the cocrystal, is free of interference from any other component
507 within the formulation. By plotting the intensity of this specific peak across the
508 the sampled cross-sectional area of the extrudate we can determine the
509 distribution of the cocrystal.

510 Figure 8 (a) provides a Raman map of the extrudate produced using only
511 cocrystal reagents devoid of any excipient. The peak intensity at 1020 cm^{-1} has
512 been used to generate the Raman map using a rainbow cubic look-up table. The
513 lookup table was generated within an ordinate range of [1000-7500 INT]. It is
514 apparent that there is a difference in the intensity of the cocrystal peak across
515 the cross-sectional area with a highly intense region focused to the outer edges
516 of the extrudate. The spectra of a number of labelled points, representing a range
517 of intensities across the map are provided for comparative purposes.

518 The mapping results shown in Figure 9 depict the intensity values of the
519 1020.50 cm^{-1} peak in extrudates containing different concentrations of xylitol
520 and following storage. Interestingly, the intensity of the cocrystal peak varied
521 considerably as a function of xylitol concentration and storage. When extruded
522 with 10% xylitol (Figure 9(1)), there was an obvious and significant increase in
523 the intensity of cocrystal (relative to neat extrusion) across the cross-sectional
524 area of the extrudate. This result correlated well with results obtained from XRD
525 where the formulations containing 10% xylitol had intense diffraction bands at
526 3.3° and 17.1°. With increasing xylitol concentration in the formulation (30%
527 and 50%, respectively), the overall intensity for the characteristic cocrystal peak

528 at 1020.50 cm⁻¹ decreased throughout the entire cross-section (Figure 9, (2) and
529 (3)). This result was again mirrored in the XRD where the cocrystal yield
530 decreased from 33.46±0.55% to 28.25±0.65%, as the concentration of xylitol
531 increased from 10% to 50%. Importantly, after 12-month storage under
532 controlled conditions (20°C with 70% RH), an extensive increase in the intensity
533 values for the distinctive cocrystal peak at 1020 cm⁻¹ was observed for all three
534 formulations containing xylitol (Figure 9, (4), (5) & (6)), suggesting significant
535 growth of the cocrystal content upon aging .

536

537 ***Cocrystal Morphology Study***

538 The crystal habit of a drug is extremely important consideration in
539 pharmaceutical manufacturing. Typically a number of basic physicochemical
540 properties such as solubility, dissolution rate, powder flow, compressibility, and
541 mechanical strength depend on the crystal habit. Figure 10 cshows polarised
542 light micrographs of Ibu, as received, cocrystal formed using traditional solvent
543 methods and melt extruded cocrytal particles. The PLM images clearly depict the
544 needle-like shape of both Ibu and the reference cocrystal standard. Such
545 anisotropic shape could be problematic during pharmaceutical manufacturing
546 ^{58,59}. Conversely, the melt-extruded cocrystal particles (Figure 10c), were
547 uniformly shape and much smaller in size.

548

549 ***In-vitro Drug Dissolution***

550 Drug release profiles (Figure 11) and associated data confirmed that all extruded
551 formulations exhibited improved solubility and increased dissolution rate of Ibu
552 with the exception of the formulation containing Eudragit® E PO. The amorphous
553 dispersion with Soluplus® (formulation 2) had a similar relative dissolution rate
554 at 5 min (0.95±0.06) and 45 min (0.44±0.04) to the neat-extruded formulation 1
555 (0.94±0.04 and 0.44±0.00, respectively). Formulation 1, however, had a
556 significantly higher dissolution rate (0.20±0.01) and increased solubility
557 (DP_{180min} of 36.30±1.33%) at 180 min than formulation 2 (0.16±0.02, and
558 29.08±3.13%, respectively). The inclusion of xylitol significantly increased the
559 dissolution rate at drug percent released. In particular, the extruded suspension
560 containing 50% w/w xylitol (formulation 6) exhibited the highest DP and RDr

561 values of all formulations (DP_{5min} at $6.41\pm 0.07\%$, DP_{45min} at $37.41\pm 0.81\%$,
562 DP_{180min} at $43.53\pm 0.34\%$, RDR_{5min} of 1.28 ± 0.01 , RDR_{45min} of 0.83 ± 0.02 and,
563 RDR_{180min} of 0.24 ± 0.00 , respectively.

564

565 ***Cocrystal Content Evaluation After Aging***

566 The stability of pharmaceutical materials that may undergo physical form change
567 during storage is fundamentally important. Stability must be examined in detail
568 in order to develop successful pharmaceutical products. The physical stability
569 relating to the relative quantity of cocrystal is shown in Figure 12. Samples were
570 stored at room temperature under both desiccated and humid conditions ($20^{\circ}C$
571 over silica gel, and $20^{\circ}C$ with 70%RH, respectively) to evaluate changes in the
572 cocrystal content. As previously presented, formulation 4 that contained 10%
573 w/w xylitol showed a significantly higher cocrystal yield ($33.46\pm 0.55\%$) than the
574 neat-extruded formulation 1 ($28.06\pm 1.65\%$) immediately after HME processing.
575 Increasing the concentration of xylitol considerably decreased the yield for
576 formulations 5 ($28.60\pm 0.61\%$) and 6 ($28.25\pm 0.65\%$), respectively. A similar but
577 qualitative indication was also evident in the Raman maps. Interestingly, the
578 neat extruded formulation 1 showed an increase in cocrystal yield increase
579 following 12-month storage under dry ($33.85\pm 2.69\%$) and humid ($43.31\pm 1.25\%$)
580 conditions, respectively. Formulations containing xylitol, retained the same
581 quantity of cocrystal yield following storage under dry conditions, while showing
582 increase to various extents, $34.86\pm 0.85\%$, $35.66\pm 1.88\%$ and 34.49 ± 2.40 for
583 formulations 4, 5 and 6, respectively, following storage under humid conditions.

584

585 **Discussion**

586 Pharmaceutical cocrystals offer a way to overcome the solubility issues
587 associated with BCS class II compounds while also retaining the thermodynamic
588 stability of the crystalline form of a drug^{60,61}. Conventionally, the manufacture of
589 a pharmaceutical cocrystal product is divided into two major aspects: the
590 production/synthesis of the cocrystal itself and the subsequent formulation of
591 cocrystal into a pharmaceutical dosage form. Pharmaceutical cocrystals have
592 developed significantly in the past decade with increasing number of patents
593 issued worldwide. However, at present there is still limited marketed examples

594 of pharmaceutical products involving cocrystals^{62,63}. With the recent
595 implementation of techniques such as hot-melt extrusion²⁸ and spray drying^{64,65},
596 as methods of manufacturing pharmaceutical cocrystals, it has become possible
597 to combine cocrystallisation and formulation to reduce the number of
598 manufacturing steps involved in drug product manufacture. Hot-melt extrusion
599 is particularly advantageous owing to its continuous processing capability; ease
600 of scaling and it may be used to manufacture cocrystals without the need for
601 organic solvents.

602 To achieve mechanochemical synthesis of cocrystals via HME comprehensive
603 investigations must be conducted in order to develop a thorough understanding
604 of the reaction selectivity between ingredients; the most appropriate reaction
605 conditions/parameter settings for a specific system; and most importantly, the
606 selection of a suitable matrix for the cocrystal reagents. To probe this further, we
607 have processed mixtures consisting of chosen cocrystal reagents and an 'inert'
608 carrier excipient via hot melt extrusion. The principal hypothesis being that
609 Ibu/IsoNA cocrystals should be suspended in the final matrix. Consequently, the
610 HME processing temperature was set significantly lower than the T_m onset of the
611 cocrystals (approximately 120°C). The chosen carrier excipient was either a
612 pharmaceutical grade polymer (Eudragit® EPO and Soluplus®) with relatively
613 low values of T_g hence lower processing temperature, or a commonly used food
614 and pharmaceutical additive, namely Xylitol, that was molten at the chosen
615 extrusion temperature.

616 For Soluplus® and EPO there was evidence of crystalline IsoNA within the
617 matrices and negligible Ibu/IsoNA cocrystal product. Moreover, for both
618 polymeric systems, there was no evidence within XRD patterns of crystalline Ibu,
619 after extrusion. In the case of Soluplus®, the lack of crystalline Ibu may be
620 attributed to heating the drug beyond its melting point during extrusion (92°C)
621 and entrapping the drug in a highly viscous polymer network. The entrapment of
622 Ibu molecules within rubbery and highly viscous Soluplus® would lead to
623 reduced mobility of Ibu and consequently reduce the interaction with IsoNA,
624 limiting cocrystal yield. Conversely, when utilising EPO as a matrix carrier,
625 competition between EPO and the cofomer isonicotinamide to form hydrogen
626 bonds with ibuprofen would further impact upon cocrystal yield. There have

627 been many reports of interactions between carboxylic acids and EPO⁶⁶⁻⁶⁸.
628 Additionally, we would expect, as with Soluplus[®], that the mixing of Ibu with
629 highly viscous rubbery EPO would physically hinder molecular interaction
630 between the cocrystal reagents limiting cocrystal yield.

631 Conversely, the small molecular weight sugar alcohol used in this study
632 (xylitol), was found to assist cocrystallization. In part, this may be attributed to
633 limited miscibility between cocrystal product and Xylitol. Indeed, polyols have
634 been shown previously to be relatively inert during extrusion⁶⁹. Furthermore, it
635 is well accepted that low molecular weight solvents (typically volatile organic
636 solvents) can significantly improve cocrystal yield. There are many reported
637 articles describing the significant increase in yield associated with solvent-
638 assisted-methods relative to neat preparation^{17,70,71}. In comparison to Soluplus[®]
639 and EPO, Xylitol is a low molecular weight (152 g/mol) carrier, with a melt
640 viscosity typically 3~4 orders of magnitude lower than the two polymeric
641 excipients. The lack of miscibility between the cocrystal and xylitol and the low
642 viscosity and hence, increased molecular mobility of cocrystal reagents appear to
643 have been key drivers in the successful production of cocrystal. Moreover, the
644 low viscosity, ease by which cocrystal may disperse throughout the melt⁵⁸ and
645 the rapid solidification of xylitol post-extrusion, led to a solid extrudate with
646 cocrystal well dispersed throughout the xylitol matrix.

647 Cocrystals formed using xylitol as a matrix carrier possessed the same
648 hydrogen-bonding pattern (FTIR) and crystal structure (XRD) as the reference
649 cocrystal manufactured via solvent evaporation and the neat-extruded cocrystal.
650 The inert nature of xylitol and the limited miscibility with the cocrystal is
651 fundamental to successful cocrystal formation during extrusion. Strong non-
652 covalent interactions between any ingredients, other than a cofomer pair, may
653 be detrimental to product formation and yield. Therefore, it becomes very
654 important to understand and if necessary quantify the strength of interaction
655 between all components to ensure successful cocrystal formation during
656 extrusion.

657 From this work, it is evident that cocrystal suspensions may be successfully
658 manufactured in a single step using extrusion provided a matrix carrier has
659 specific qualities. Potential matrix carriers should have limited ability to form

660 non-covalent interactions with all cocrystal components, a sufficiently low
661 processing temperature such that it is lower than cocrystal melting temperature
662 and rapid solidification upon cooling.

663 The improvement in the dissolution of drug compounds, when manufactured
664 as cocrystals, can be used to enhance the solubility of BCS class II drugs. It was
665 evident that the addition of small quantities of xylitol (10%) increased cocryatl
666 yield however at higher xylitol concentrations (30% and 50%), the cocrystal
667 yield was equivalent to the formulation devoid of xylitol (Formulation 1). There
668 was no evidence of crystalline ibuprofen immediately after processing, indicating
669 that residual ibuprofen was rendered amorphous. Therefore, the amorphous
670 content (as percentage of the total Ibu content) in the 30% and 50% xylitol
671 formulations were equivalent to that in the neat-extruded formulation. And the
672 amorphous Ibu content in the 10% xylitol formulation was less than that in the
673 system devoid of xylitol.

674 In drug dissolution studies, formulation 1 (devoid of xylitol) exhibited
675 significantly increased rate and extent of drug release relative to the crystalline
676 ibuprofen powder. This could be the result of a combined effect of the formation
677 of both the cocrystal and amorphous forms of ibuprofen. Although it is difficult
678 to quantify the impact of each individual form to the dissolution improvement,
679 the fact that formulations 1, 5 and 6 all had equivalent amounts of cocrystal yield
680 is suggesting that the further increased dissolution rates of formulations 5 and 6,
681 relative to formulation 1, are attributed to the presence of xylitol.

682 The enhanced dissolution rate observed for a cocrystal suspension embedded
683 in a hydrophilic matrix relative to neat cocrystal powders may be attributed to
684 (1) the cocrystal particles present in the suspension are less aggregated due to
685 the distribution within the matrix carrier, facilitated by agitation caused by
686 extrusion screw rotation and (2) improved wettability owing to the
687 hydrophilicity of the carrier^{42,72-75}. For the matrix containing Soluplus®, the
688 release of Ibu initiated rapidly due to the presence of amorphous Ibu at the
689 surface of the Soluplus® matrix. However, the erosion of the Soluplus® matrix
690 was significantly slower than that of formulations containing xylitol or those
691 devoid of excipient. With IsoNA rapidly dissolving into the dissolution medium
692 due to its high aqueous solubility, the rapid ingress of water into the Soluplus®

693 matrix may have increased Ibu mobility causing clustering of the dispersed Ibu
694 molecules and their subsequent recrystallization within the matrix. Conversely,
695 the formulation containing EPO, exhibited a reduced dissolution rate. This
696 retardation of drug release may be due to the cationic nature of the polymer, the
697 interaction with the acidic drug and the inherent slow dissolution of the
698 polymeric carrier in the chosen dissolution media.

699 Many approaches have been used to enhance the dissolution performance of
700 BCS class II drugs. Cocrystals have not only been shown to improve drug release
701 properties but are also more physically stable than amorphous drug forms
702 during storage. To understand the storage stability of the extrudates cocrystal
703 suspensions were desiccated under two different conditions, namely, a dry
704 environment over silica gel, and humid condition maintained at 70%RH, both at
705 20°C for 12 months. As previously discussed, hydrogen bonds between the two
706 cocrystal reagents are stronger than that between the homo-molecules^{6,41}, it is
707 therefore of relevance to confirm if the formed cocrystal could stay unchanged
708 under pharmaceutically relevant storage conditions. Indeed, both Raman
709 mapping and PXRD patterns showed that the stored samples had varying
710 degrees of cocrystal growth as a result of aging. This is quantitatively indicative
711 of incomplete cocrystallisation during extrusion. However, both DSC and PXRD
712 analyses on extrudates immediately following manufacture showed little
713 evidence of the presence of crystalline Ibu or IsoNA. The growth of cocrystal
714 during storage may be attributed to interaction between amorphous Ibu and
715 IsoNA molecules, that subsequently form cocrystals⁷⁶. The samples stored under
716 high humidity, in particular, showed significant cocrystal growth during storage
717 most probably due to increased global molecular mobility following ingress of
718 moisture into the xylitol matrix. Consequently, it may be concluded that even if
719 reagents are partially amorphous following extrusion and are physically
720 stabilised by the presence of a matrix carrier they may still recrystallize. This is
721 driven by the ingress of moisture, the drop in T_g, associated increase in
722 molecular mobility of the amorphous components⁷⁷ and the subsequent
723 formation of a thermodynamically favourable cocrystal product.

724 Furthermore, the incomplete cocrystal conversion may be attributed to the
725 rapid transport of material through the extrusion barrel, limiting reaction time.

726 The residence time of a typical HME process is a multifactorial-controlled
727 variable that is dependent upon factors such as the properties of the extruded
728 materials, the processing parameter settings and, the machine geometry⁷⁸⁻⁸². For
729 larger scale extruders, residence time may be prolonged due to physically
730 extended barrel length. Limitation with respect to limited reaction time may be
731 overcome using increased mixing intensity. An incorrect choice of screw
732 geometry may lead to inadequate mixing in the barrel and reduce cocrystal
733 yield^{27,28}. The extruder utilized in this work consisted of a 10cm long conical
734 barrel coupled with non-intermeshing conical co-rotating screws. A full
735 conveying screw design was employed throughout the entire length of the
736 barrel. With this set-up, the compression of materials occurs by decreasing the
737 barrel volume in the direction of melt flow. When extruding a cocrystal
738 suspension from a mixture of the reagent pair and a chosen carrier, however,
739 such an extruder design (limited mixing intensity) may not be aggressive enough
740 to compensate for the limited residence time. In addition, it may also be
741 important to consider the solubility of cocrystal parent reagents in the carrier. A
742 liquefied carrier that cannot solubilize the parent reagents may reduce
743 interspecies collision. Conversely, carrier-reagent reactivity should be less than
744 reagent-reagent reactivity in order to encourage increased cocrystal yield.
745 Theoretically, the solubility of the components within this process would be
746 expected to be temperature dependent. Thus a detailed investigation into the
747 influence of processing temperature on the solubility between components and
748 hence the cocrystal conversion is necessary.

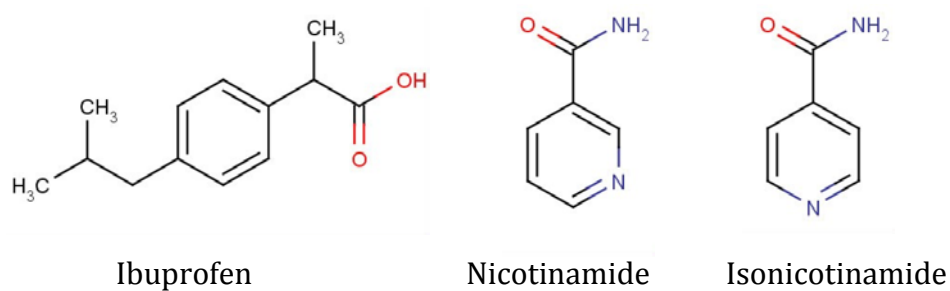
749

750 **Conclusion**

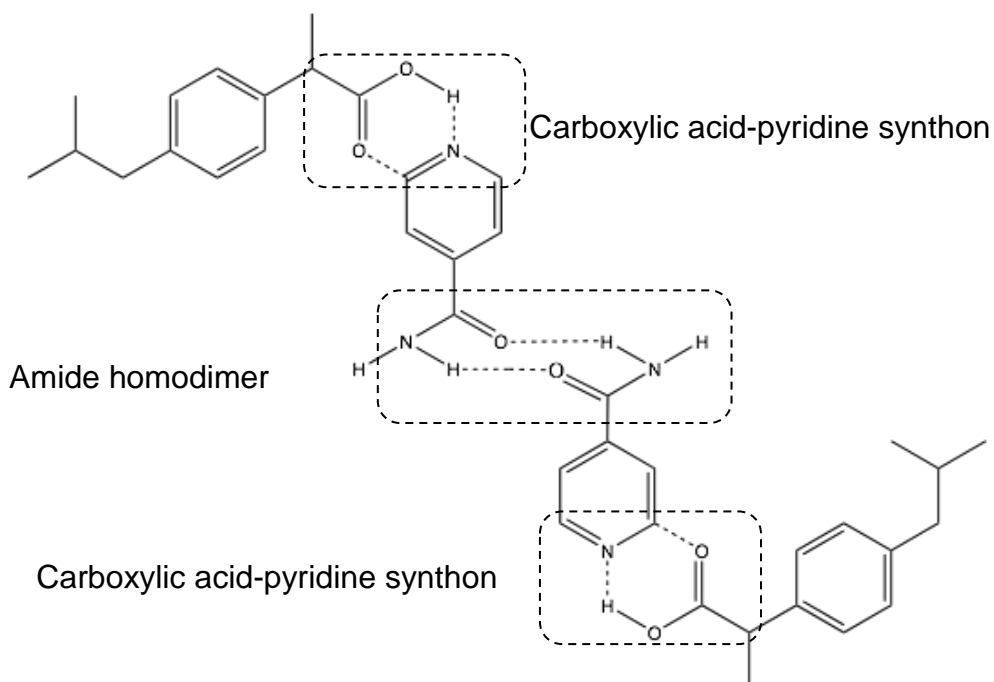
751 This work demonstrated the viability of concurrent cocrystallisation and drug
752 product formulation in a miniature scale (10g) co-rotating twin-screw extruder.
753 The final extrudates were examined to be intimate mixtures wherein the newly
754 formed cocrystal particulates were physically suspended in a matrix formed by a
755 'inert' carrier excipient. Importantly, it was established in this study that an
756 appropriate carrier for a cocrystal reagent pair during HME processing should
757 satisfy certain criteria including: (1) limited interaction with parent reagents and
758 cocrystal product; (2) processing temperature sufficiently lower than the onset

759 of cocrystal T_m ; (3) low melting viscosity; and (4) fast solidification upon cooling.
760 In conclusion, the use of low viscosity, chemically 'inert' matrix carriers may be
761 successfully employed in the mechanochemical synthesis of pharmaceutical
762 cocrystal suspensions via HME.

Figures



(a)



(b)

Figure 1(a). Molecular structure of Ibuprofen, nicotinamide, isonicotinamide and **(b)** proposed theoretical architecture of an ibuprofen/IsoNA cocrystal (Frišćić & Jones 2007, Karki et al; 2007). Hydrogen bonds are shown as dotted lines.

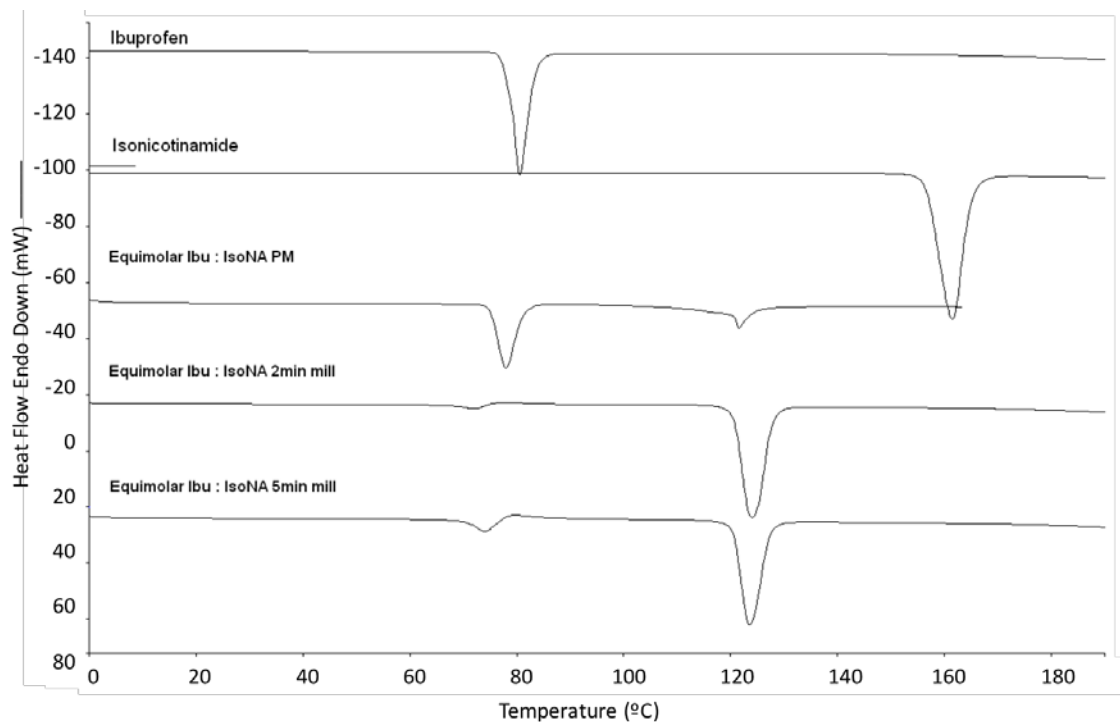


Figure 2 Representative DSC thermogram from top to bottom: crystalline ibuprofen; crystalline isonicotinamide (as is); physical mixture (PM) of ibuprofen & isonicotinamide at 1:1 molar ratio; equimolar Ibu/IsoNA ball milled for 2 minutes; and equimolar Ibu/IsoNA ball milled for 5 minutes.

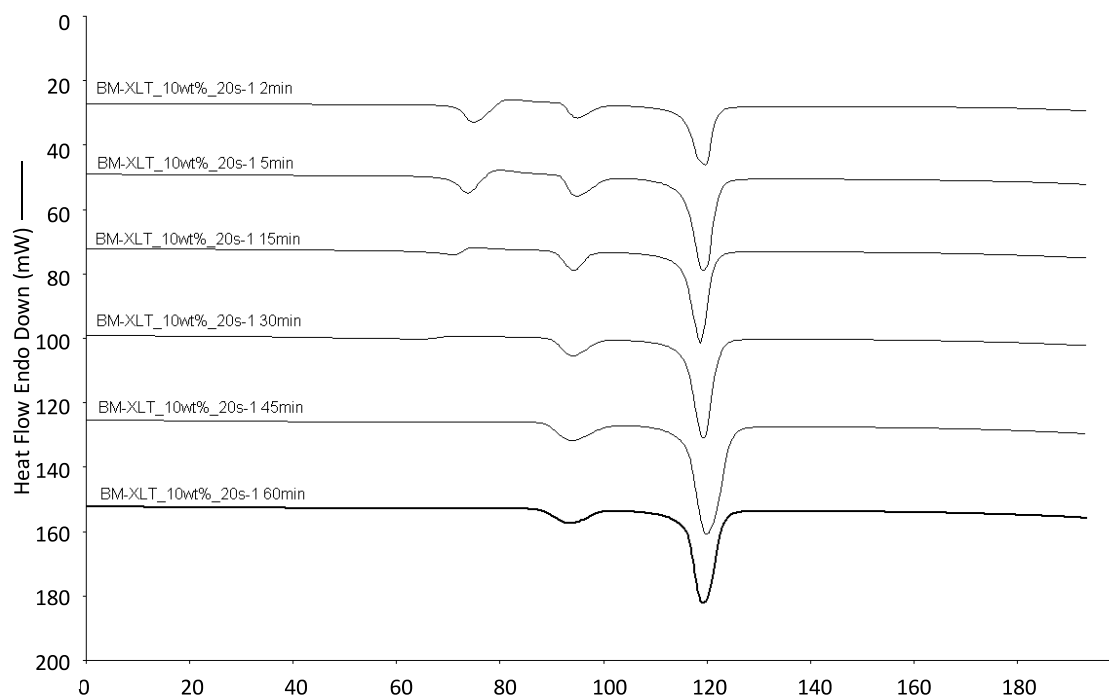


Figure 3 Overlaid DSC thermograms showing the formation and increase of Ibu/IsoNA cocrystal in the presence of 10wt% xylitol after (from top to bottom): 2, 5, 15, 30, 45 and, 60 minutes ball milling.

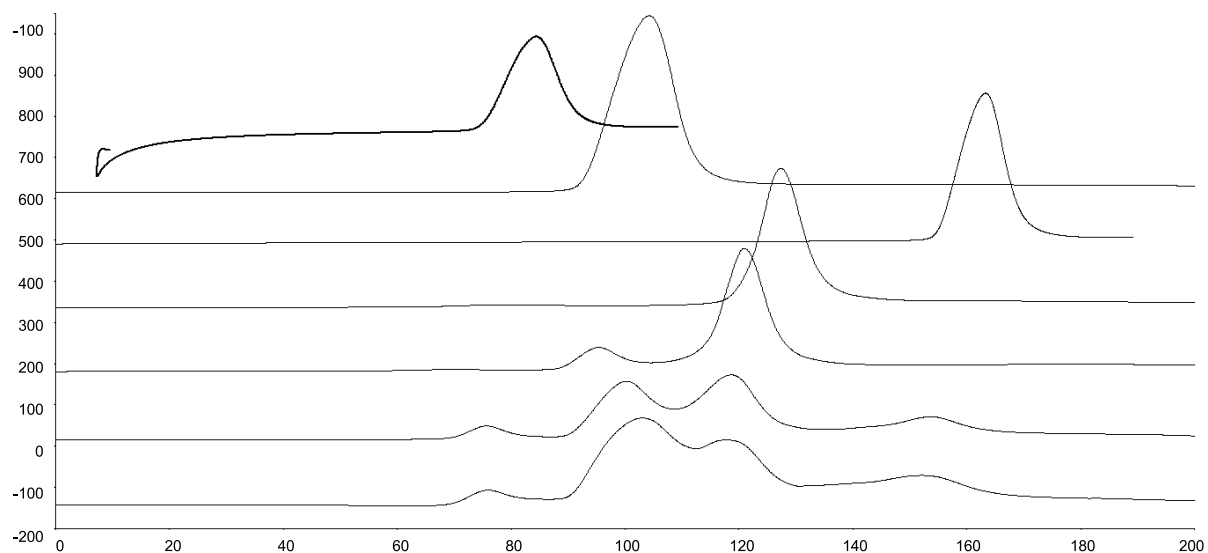


Figure 4 Representative DSC thermograms of materials used in cocrystal formulation development. From top to bottom: ibuprofen, xylitol, isonicotinamide, reference cocrystal standard prepared using solution method, extruded Ibu/IsoNA cocrystal suspension in 10wt% xylitol; extruded Ibu/IsoNA cocrystal suspension in 30wt% xylitol and, extruded Ibu/IsoNA cocrystal suspension in 50wt% xylitol.

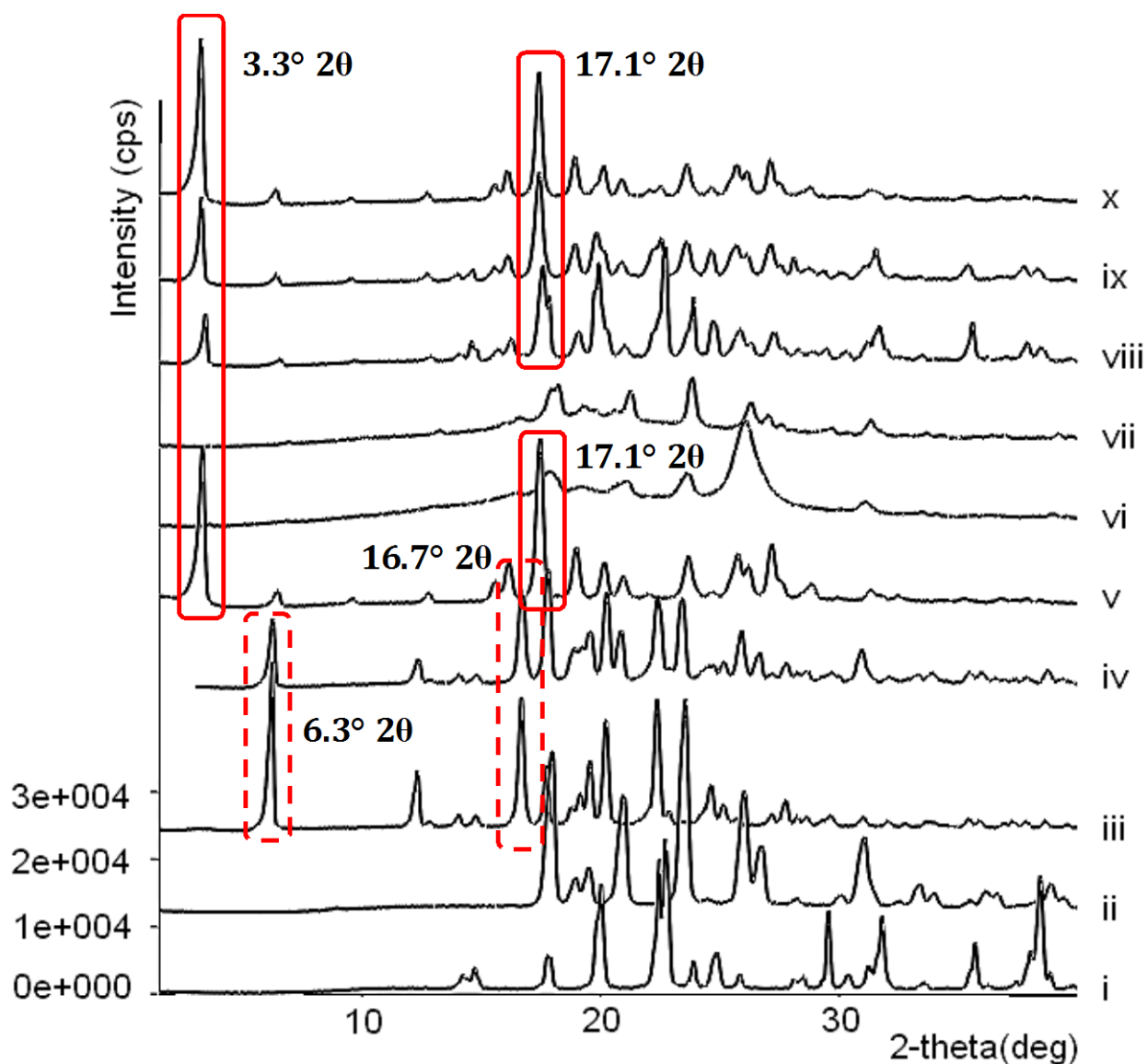


Figure 5 Overlaid PXRD patterns of: (i) xylitol; (ii) IsoNA; (iii) Ibu; (iv) equimolar Ibu/IsoNA physical mixture; (v) 1:1 neat extruded at 92°C; (vi) 10wt% Soluplus® HME; (vii) 10wt% EPO HME; (viii) 50wt% xylitol HME; (ix) 30wt% xylitol HME; and (x) 10wt% xylitol HME. Please note: all extrudates contained ibuprofen and isonicotinamide at a 1:1 molar ratio.

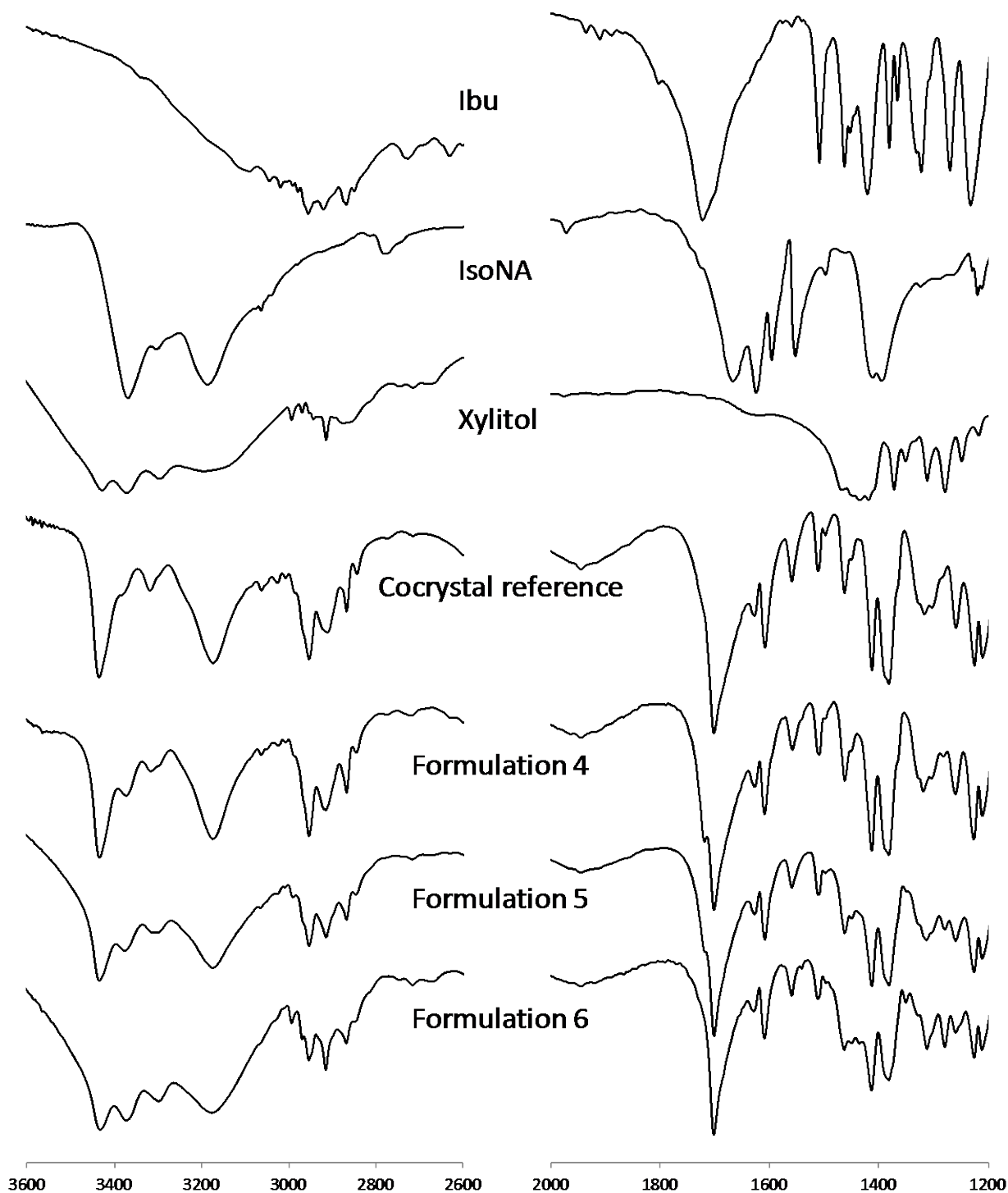


Figure 6 Overlaid FTIR spectra within wavenumber ranges of [2600-3600 cm^{-1}] and [1200-2000 cm^{-1}], respectively for, from top to bottom: Ibu, IsoNA, xylitol, the coccrystal reference, extruded suspensions containing 10%, 30% and, 50% xylitol, respectively.

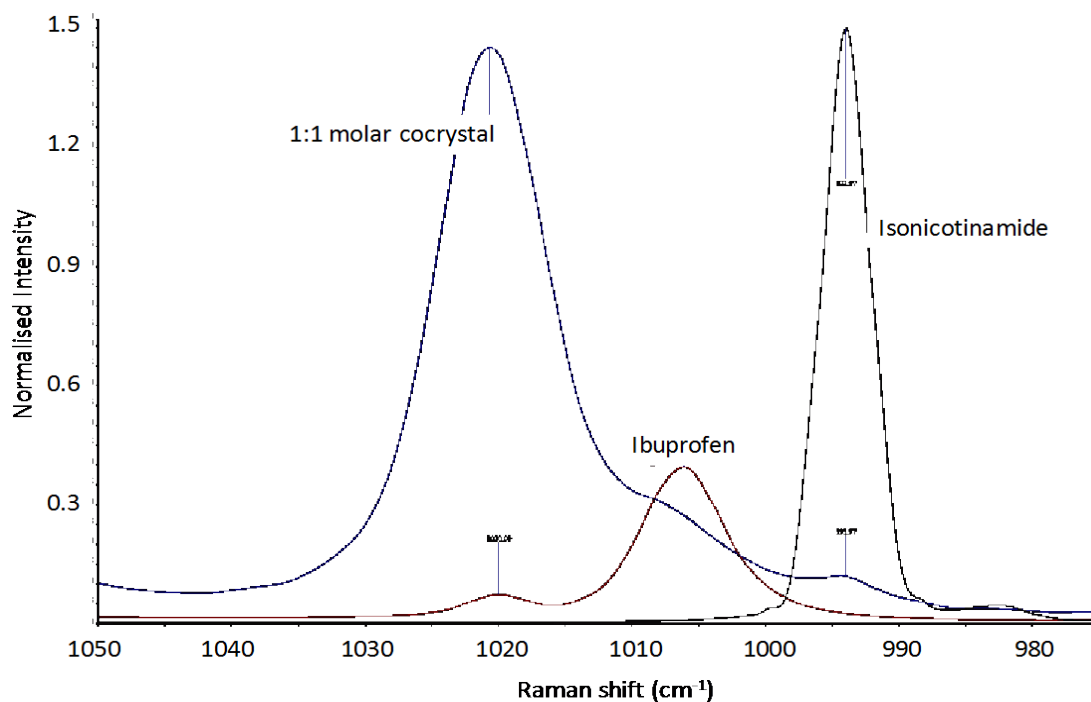


Figure 7 Raman shift region [1050.0~975.0 cm⁻¹] showing non-interfering, characteristic peaks for: (Red) unprocessed Ibuprofen; (green) unprocessed IsoNA; and (blue) the equimolar cocrystal prepared using slow evaporation.

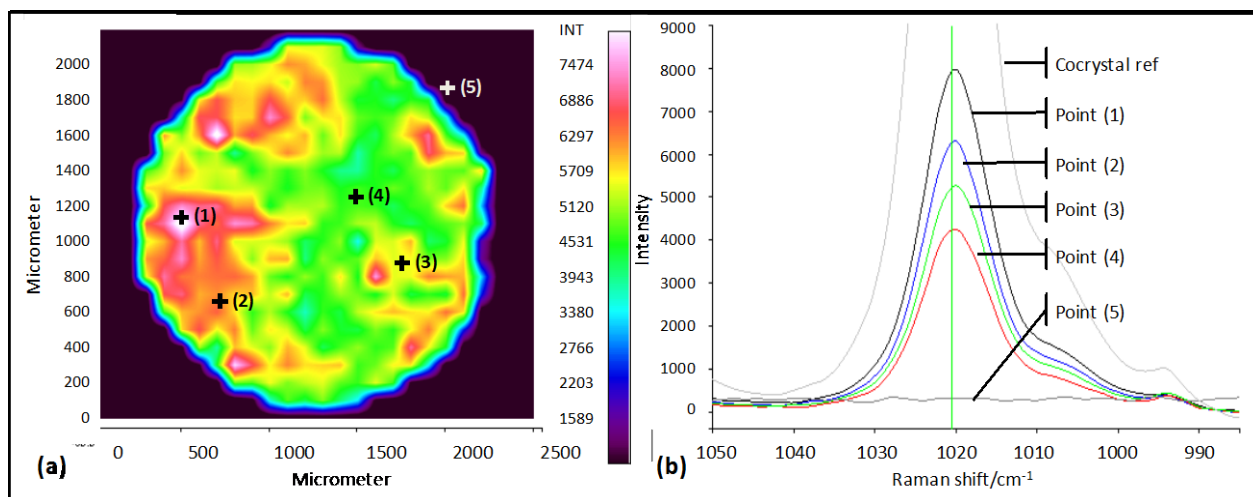


Figure 8 (a) Schematic demonstration of the occurrence and concentration of the cocrystal across the cross section of a formulation 1 extrudate. **(b)** The spectra showing the intensity of the cocrystal peak at 1020 cm⁻¹ at the labelled points and that of the cocrystal reference are shown in the right figure in an overlaid format.

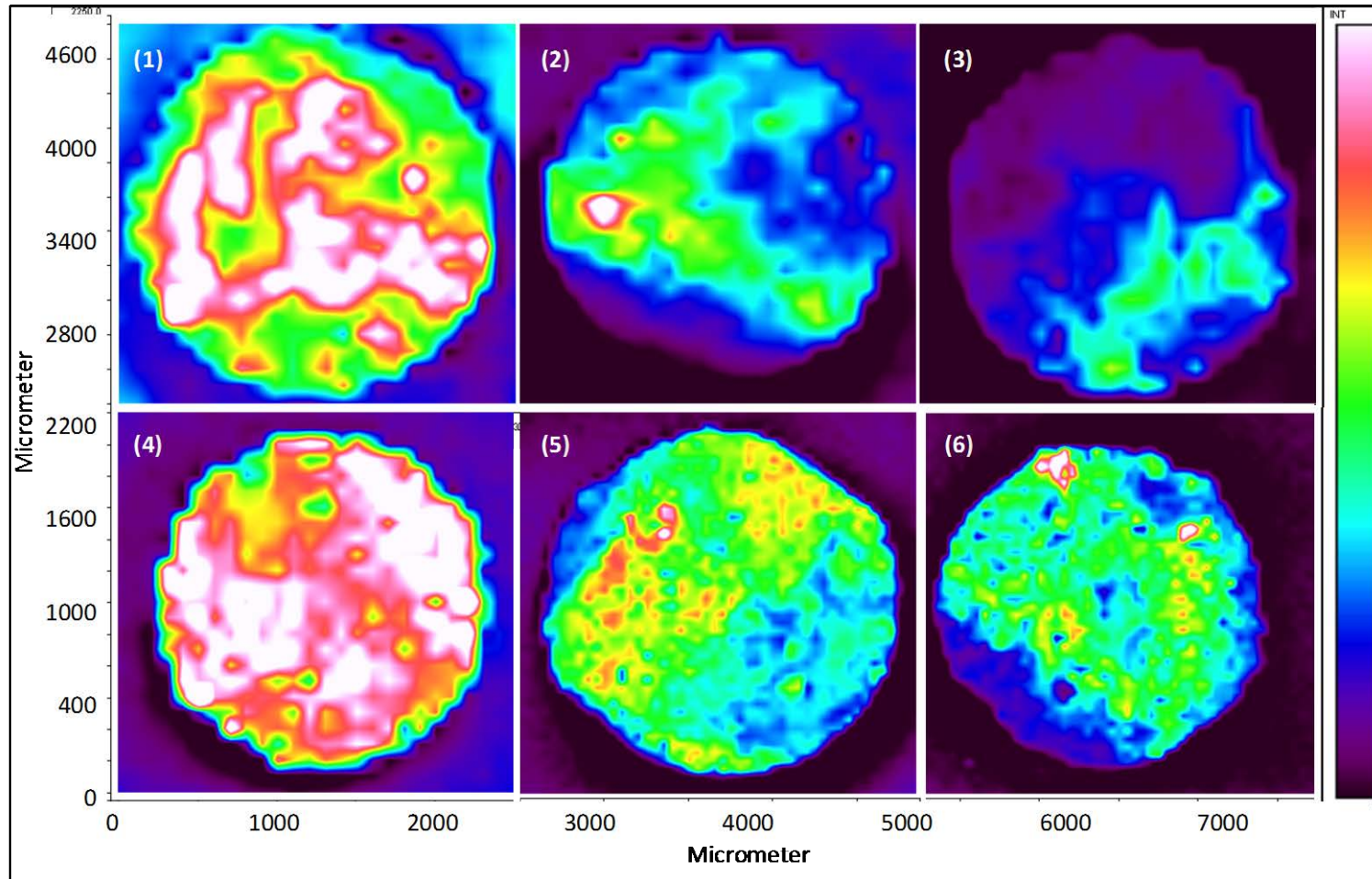


Figure 9 Raman map/image showing the intensity of the peak at 1020 cm^{-1} , characteristic of the cocrystal, throughout the cross section of: (1) fresh extrudates of formulation 4, containing 10% xylitol; (2) fresh extrudates of formulation 5, containing 30% xylitol; (3) fresh extrudates of formulation 6, containing 50% xylitol; (4) aged formulation 4; (5) aged formulation 5; and (6) aged formulation 6.

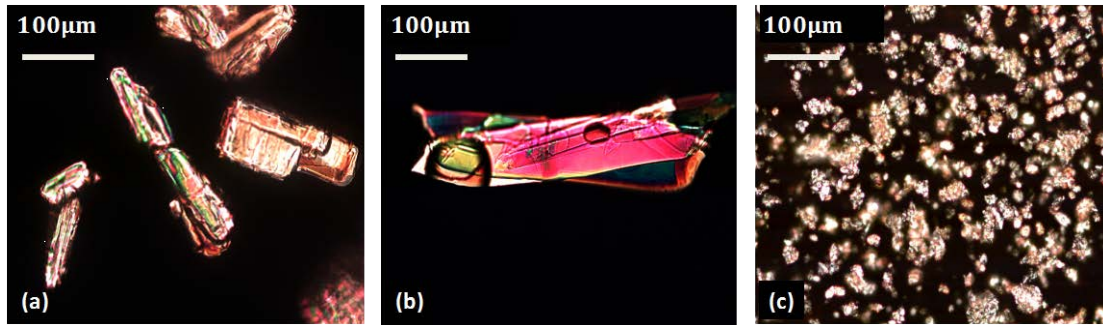


Figure 10 Polarized light micrographs showing crystal habit and size of: **(a)** unprocessed Ibu; **(b)** reference 1:1 Ibu/IsoNA cocrystal prepared using solvent evaporation; and **(c)** melt-extruded cocrystal particles. Particulates chosen all passed through 212µm sieve and were dispersed in mineral oil (200x, the entire width of each picture represents 0.5mm on a magnified scale bar).

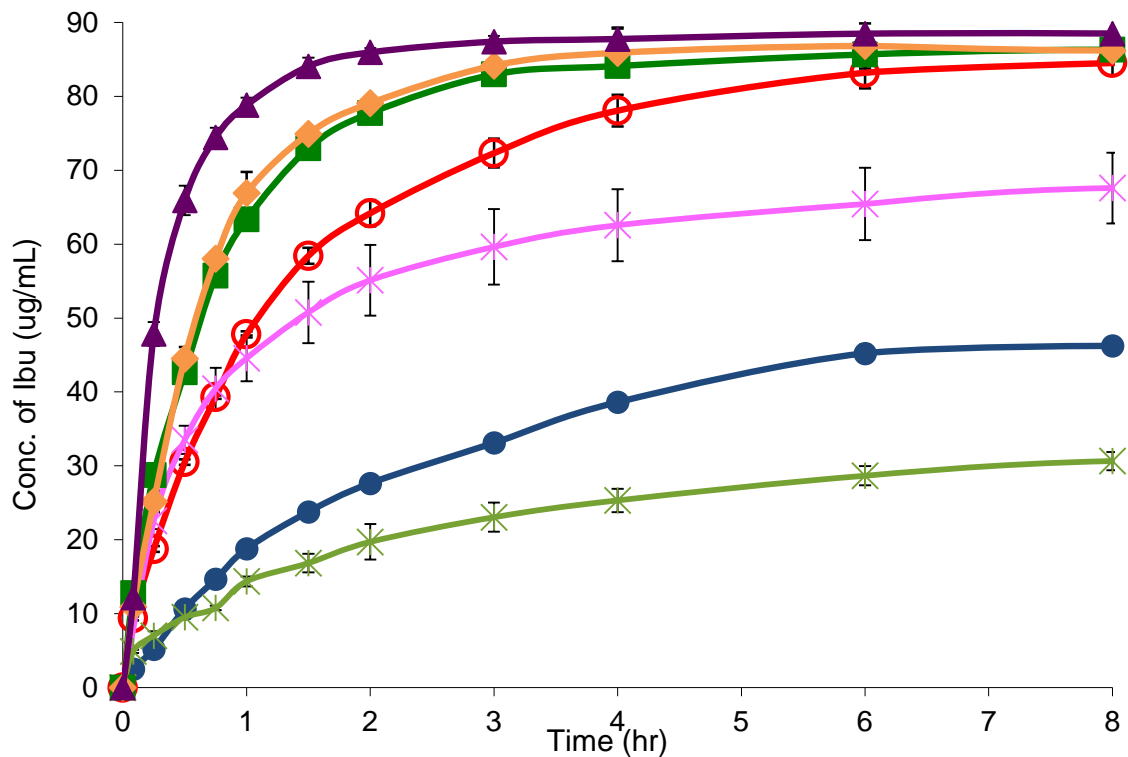


Figure 11 Drug dissolution profiles of melt extruded equimolar Ibu/IsoNA formulations in deionized water. Profiles from bottom to top: (*) extrudates containing Eudragit® EPO; (●) Pure ibuprofen powders; (*) extrudates containing Soluplus®; (○) 1:1 melt-extruded cocrystal (formulation 1); (■) 1:1 extruded cocrystal suspension in 10% xylitol (formulation 4); (◆) 1:1 extruded cocrystal suspension in 30% xylitol (formulation 5); and (▲) 1:1 extruded cocrystal suspension in 50% xylitol (formulation 6). Each point represents the mean \pm S.D. of 3 replicates.

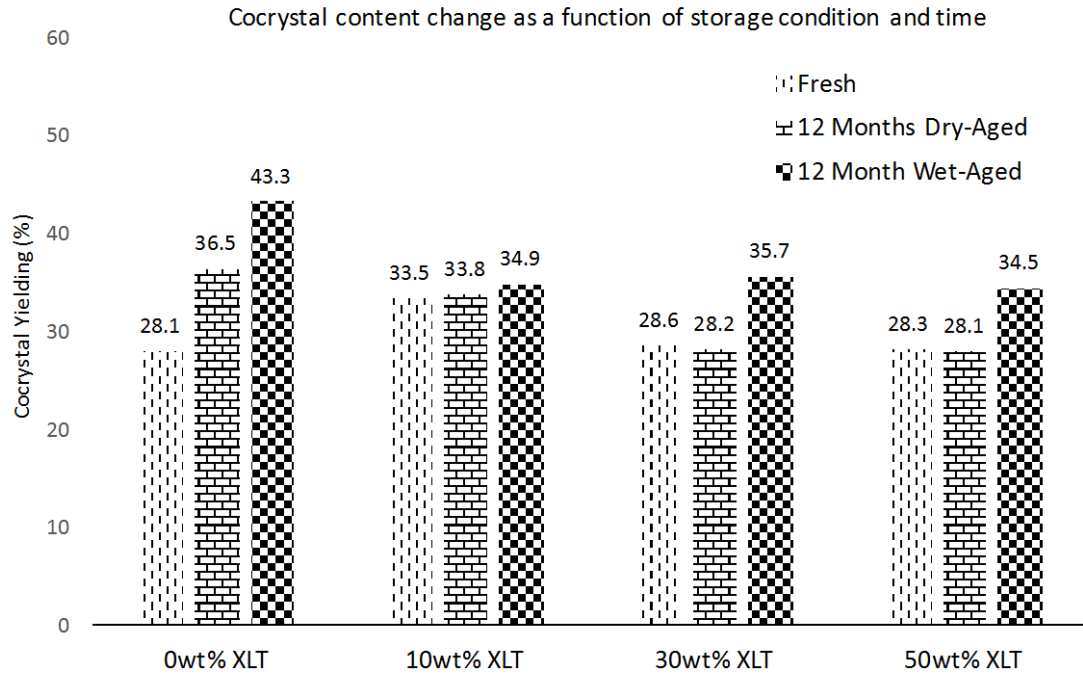


Figure 12 Yielded cocrystal content determination for freshly extruded and stored cocrystal suspension formulations containing (from left to right): 0%, 10%, 30% and, 50%, w/w xylitol.

Tables

Table 1 Nomenclature and the Parameter Settings for the Hot-Melt Extruded Formulations Composed of Equimolar Ibu and IsoNA, as well as a Third Matrix Carrier. ^a

Formula	Ibu wt%	IsoNA wt%	Soluplus® wt%	Eudragit® EPO wt%	Xylitol wt%	Feed & Mix Temp/speed °C /rpm	Flushing Temp/speed °C /rpm	Residence time s	Flush Torque Ncm	Outcome
1	62.82	37.18	–	–	–	92/10	92/10	233	40~44	Fragile rods
2	56.54	33.46	10	–	–	92/10	92/10	241	4~6	Sticky strand
3	56.54	33.46	–	10	–	92/10	92/10	220	4~6	Sticky strand
4	56.54	33.46	–	–	10	92/10	85/50	90	109~122	Brittle strand
5	43.98	26.02	–	–	30	92/10	85/50	272	43~59	Brittle strand
6	31.41	18.59	–	–	50	92/10	85/50	329	19~22	Brittle strand

^a Note that the weight ratios tabulated here provide 1:1 molar ratio for Ibu and IsoNA in the blends. The batch size was maintained at approximately 10g for each formulation and the extrudates were collected after equilibration for 5 minutes.

Table 2. The Molecular Weights, Melting/Glass Transition Temperatures and Decomposition Temperatures of Each Individual Compound used in This Study. ^a

Compound	Mw g/mol	T_m or T_g °C	T_{5wt% loss} °C
Ibu	206.30	84.41 ± 0.57	197.44 ± 3.67
IsoNA	122.12	163.26 ± 0.99	188.10 ± 2.14
Ibu/IsoNA cocrystal	656.48	127.29 ± 0.55	164.07 ± 6.77
Xylitol	152.15	104.17±0.29	270.03 ± 0.43
Eudragit® E PO	47,000	43.94 ± 0.13	279.70 ± 1.00
Soluplus®	90,000~140,000	66.52 ± 0.20	308.57 ± 0.91

^a The temperatures shown here represent the mean ± SD of three replicates. Note that the values of T_m listed the peak maximums measured at 200°C/min.

Table 3 Assignment for the Most Characteristic Vibrational Bands of Ibu and IsoNA in the Raw Materials and the 1:1 Melt-Extruded Ibu/IsoNA Cocrystal.

	IR Frequency (cm⁻¹)	Raman Shift (cm⁻¹)	Band assignment ^a
Ibuprofen	3400~2800	-	ν_{O-H} (Associated)
	1721.16 (vs)	1605.95	$\nu_{C=O}$ (Carboxylic acid)
	1007.62 (m)	1006.13	ν_{C-C} (Aromatic ring chain vib)
	796.457 (m)	-	γ_{C-H} (Aromatic ring)
Isonicotinamide	3369.03 (vs)	3070.09	ν_{N-H} (Asymmetric stretching)
	3185.83 (vs)	3063.81	ν_{N-H} (Symmetric stretching)
	1668.12 (vs)	1601.58	$\nu_{C=O}$ (Stretching)
	1622.80 (s)	-	δ_{N-H} (H-bonded amide bending)
	1594.84 (m)	-	δ_{N-H} (Free amide bending)
	1551.45 (m)	993.94	ν_{Ring} (Pyridine ring stretching)
Equimolar Ibu/IsoNA reference cocrystal	3434.60 (vs)	-	ν_{N-H} (Free amide)
	3317.93 (w)	-	ν_{N-H} (H-bonded pyridine N)
	3174.26 (vs)	-	ν_{N-H} (H-bonded amide)
	1702.84 (vs)	1612.66	$\nu_{C=O}$ (Carboxylic acid)
	1629.55 (m)	-	$\nu_{C=O}$ (H-bonded amide C=O)
	1609.31 (s)	-	δ_{N-H} (Free amide)
	1560.13 (m)	1020.70	ν_{Ring} (Pyridine)
	779.101 (m)	-	γ_{C-H} (H-bonded pyridine =C-H)

^a ν = stretching vibration; δ = in-plane bending; γ = out-plane bending.

Table 4 Dissolution Parameters Calculated for Fig 11.

Formulation	Dissolution Parameters					
	DP _{5min} ^a	DP _{45min} ^a	DP _{180min} ^a	RDr _{5min} ^b	RDr _{45min} ^b	RDr _{180min} ^b
● Pure Ibu	1.26±0.17%	7.35±0.12%	16.65±0.03%	0.25±0.03	0.16±0.00	0.09±0.00
○ 1	4.69±0.19%	19.71±0.06%	36.30±1.33%	0.94±0.04	0.44±0.00	0.20±0.01
* 2	4.73±0.32%	19.83±1.71%	29.08±3.13%	0.95±0.06	0.44±0.04	0.16±0.02
* 3	2.45±0.10%	5.47±0.08%	11.64±1.36%	0.49±0.02	0.12±0.00	0.06±0.01
■ 4	5.09±0.70%	27.88±0.06%	41.90±0.04%	1.02±0.14	0.62±0.00	0.23±0.00
◆ 5	5.40±0.08%	28.74±0.18%	41.55±0.03%	1.08±0.02	0.64±0.00	0.23±0.00
▲ 6	6.41±0.07%	37.41±0.81%	43.53±0.34%	1.28±0.01	0.83±0.02	0.24±0.00

^a DP: Drug percent (%) released at a particular time point;

^b RDr: Relative dissolution rate (%/ minutes) at a particular time point. (RDr=DP/dissolution time).

References

- (1) McNamara, D.; Childs, S.; Giordano, J.; Iarriccio, A.; Cassidy, J.; Shet, M.; Mannion, R.; O'Donnell, E.; Park, A. Use of a Glutaric Acid Cocrystal to Improve Oral Bioavailability of a Low Solubility API. *Pharm. Res.* **2006**, *23* (8), 1888–1897.
- (2) Blagden, N.; de Matas, M.; Gavan, P. T.; York, P. Crystal Engineering of Active Pharmaceutical Ingredients to Improve Solubility and Dissolution Rates. *Drug Solubility How to Meas. it, How to Improv. it* **2007**, *59* (7), 617–630.
- (3) Jung, M.-S.; Kim, J.-S.; Kim, M.-S.; Alhalaweh, A.; Cho, W.; Hwang, S.-J.; Velaga, S. P. Bioavailability of Indomethacin-Saccharin Cocrystals. *J. Pharm. Pharmacol.* **2010**, *62* (11), 1560–1568.
- (4) Mohammad, M. A.; Alhalaweh, A.; Velaga, S. P. Hansen Solubility Parameters as a Tool to Predict Cocrystal Formation. *Int. J. Pharm.* **2011**, *407*, 63–71.
- (5) Qiao, N.; Li, M.; Schlindwein, W.; Malek, N.; Davies, A.; Trappitt, G. Pharmaceutical Cocrystals: An Overview. *Int. J. Pharm.* **2011**, *419*, 1–11.
- (6) Vishweshwar, P.; McMahon, J. A.; Bis, J. A.; Zaworotko, M. J. Pharmaceutical Co-Crystals. *J. Pharm. Sci.* **2006**, *95* (3), 499–516.
- (7) Thakuria, R.; Delori, A.; Jones, W.; Lipert, M. P.; Roy, L.; Rodríguez-Hornedo, N. Pharmaceutical Cocrystals and Poorly Soluble Drugs. *Int. J. Pharm.* **2013**, *453* (1), 101–125.
- (8) Basavoju, S.; Boström, D.; Velaga, S. Indomethacin–Saccharin Cocrystal: Design, Synthesis and Preliminary Pharmaceutical Characterization. *Pharmaceutical Research*. Springer Netherlands 2008, pp 530–541.
- (9) Leysens, T.; Tumanova, N.; Robeyns, K.; Candoni, N.; Veessler, S. Solution Cocrystallization, an Effective Tool to Explore the Variety of Cocrystal Systems: Caffeine/dicarboxylic Acid Cocrystals. *Cryst. Eng. Commun.* **2014**, *16*, 9603–9611.
- (10) Trask, A. V.; Jones, W. Crystal Engineering of Organic Cocrystals by the Solid-State Grinding Approach. *Topics in Current Chemistry*. 2005, pp 41–70.
- (11) James, S. L.; Adams, C. J.; Bolm, C.; Braga, D.; Collier, P.; Friscic, T.; Grepioni, F.; Harris, K. D. M.; Hyett, G.; Jones, W.; Krebs, A.; Mack, J.; Maini, L.; Orpen, A. G.; Parkin, I. P.; Shearouse, W. C.; Steed, J. W.; Waddell, D. C.; Friščić, T.; Grepioni, F.; Harris, K. D. M.; Hyett, G.; Jones, W.; Krebs, A.; Mack, J.; Maini, L.; Orpen, A. G.; Parkin, I. P.; Shearouse, W. C.; Steed, J. W.; Waddell, D. C. Mechanochemistry: Opportunities for New and Cleaner Synthesis. *Chem. Soc. Rev.* **2012**, *41* (1), 413–447.
- (12) Delori, A.; Friscic, T.; Jones, W.; Friščić, T.; Jones, W. The Role of Mechanochemistry and Supramolecular Design in the Development of Pharmaceutical Materials. *CrystEngComm* **2012**, *14* (7), 2350–2362.
- (13) Jones, W.; Eddleston, M. D. Introductory Lecture: Mechanochemistry, a Versatile Synthesis Strategy for New Materials. *Faraday Discuss.* **2014**, *170* (0), 9–34.
- (14) Boldyrev, V. V. Mechanochemistry and Mechanical Activation of Solids. *Russ. Chem. Rev.* **2006**, *75* (3), 177–189.
- (15) Braga, D.; Grepioni, F. Solventless Reactions: Reactions between or within Molecular Crystals. *Angew. Chemie, Int. Ed.* **2004**, *43* (31), 4002–4011.
- (16) Shan, N.; Toda, F.; Jones, W. Mechanochemistry and Co-Crystal Formation: Effect of Solvent on Reaction Kinetics. *Chem. Commun.* **2002**, No. 20, 2372–2373.

- (17) Trask, A. V; Motherwell, W. D. S.; Jones, W. Solvent-Drop Grinding: Green Polymorph Control of Cocrystallisation. *Chem. Commun.* **2004**, No. 7, 890–891.
- (18) Friščić, T.; Fabian, L.; Burley, J. C.; Jones, W.; Motherwell, W. D. S. Exploring Cocrystal-Cocrystal Reactivity via Liquid-Assisted Grinding: Assembling of Racemic and Dismantling of Enantiomeric Cocrystals. *Chem. Commun.* **2006**, 28 (48), 5009–5011.
- (19) Friščić, T.; Trask, A. V; Jones, W.; Motherwell, W. D. S. Screening for Inclusion Compounds and Systematic Construction of Three-Component Solids by Liquid-Assisted Grinding. *Angew. Chemie* **2006**, 118 (45), 7708–7712.
- (20) Friščić, T.; Childs, S. L.; Rizvi, S. A. A.; Jones, W. The Role of Solvent in Mechanochemical and Sonochemical Cocrystal Formation: A Solubility-Based Approach for Predicting Cocrystallisation Outcome. *Cryst. Growth Des.* **2009**, 11 (3), 418–426.
- (21) Yamamoto, K.; Tsutsumi, S.; Ikeda, Y. Establishment of Cocrystal Cocktail Grinding Method for Rational Screening of Pharmaceutical Cocrystals. *Int. J. Pharm.* **2012**, 437 (1-2), 162–171.
- (22) Shevchenko, A.; Miroshnyk, I.; Pietilä, L.-O.; Haarala, J.; Salmia, J.; Sinervo, K.; Mirza, S.; van Veen, B.; Kolehmainen, E.; Yliruusi, J. Diversity in Itraconazole Cocrystals with Aliphatic Dicarboxylic Acids of Varying Chain Length. *Cryst. Growth Des.* **2013**, 13 (11), 4877–4884.
- (23) Lin, Y.; Yang, H.; Yang, C.; Wang, J. Preparation, Characterization, and Evaluation of Dipfluzine–Benzoic Acid Co-Crystals with Improved Physicochemical Properties. *Pharm. Res.* **2013**, 1–13.
- (24) Sowa, M.; Ślepokura, K.; Matczak-Jon, E. A 1:1 Pharmaceutical Cocrystal of Myricetin in Combination with Uncommon Piracetam Conformer: X-Ray Single Crystal Analysis and Mechanochemical Synthesis. *J. Mol. Struct.* **2014**, 1058, 114–121.
- (25) Madusanka, N.; Eddleston, M. D.; Arhangel'skis, M.; Jones, W. Polymorphs, Hydrates and Solvates of a Co-Crystal Of caffeine with Anthranilic Acid. *Cryst. Eng.* **2014**, 70 (1), 72–80.
- (26) Friščić, T.; Jones, W. Cocrystal Architecture and Properties: Design and Building of Chiral and Racemic Structures by Solid–solid Reactions. *Faraday Discuss.* **2007**, 136, 167–178.
- (27) Medina, C.; Daurio, D.; Nagapudi, K.; Alvarez-Núñez, F. Manufacture of Pharmaceutical Co-Crystals Using Twin Screw Extrusion: A Solvent-Less and Scalable Process. *J. Pharm. Sci.* **2010**, 99 (4), 1693–1696.
- (28) Dhupal, R.; Kelly, A.; York, P.; Coates, P.; Paradkar, A. Cocrystallization and Simultaneous Agglomeration Using Hot Melt Extrusion. *Pharm. Res.* **2010**, 27 (12), 2725–2733.
- (29) Daurio, D.; Medina, C.; Saw, R.; Nagapudi, K.; Alvarez-Núñez, F. Application of Twin Screw Extrusion in the Manufacture of Cocrystals, Part I: Four Case Studies. *Pharmaceutics* **2011**, 3, 582–600.
- (30) Kelly, A. L.; Gough, T.; Dhupal, R. S.; Halsey, S. A.; Paradkar, A. Monitoring Ibuprofen–nicotinamide Cocrystal Formation during Solvent Free Continuous Cocrystallization (SFCC) Using near Infrared Spectroscopy as a PAT Tool. *Int. J. Pharm.* **2012**, 426 (1–2), 15–20.
- (31) Kulkarni, C.; Wood, C.; Kelly, A. L.; Gough, T.; Blagden, N.; Paradkar, A. Stoichiometric Control of Co-Crystal Formation by Solvent Free Continuous

- Co-Crystallization (SFCC). *Cryst. Growth Des.* **2015**, *15* (12), 5648–5651.
- (32) Remenar, J. F.; Peterson, M. L.; Stephens, P. W.; Zhang, Z.; Zimenkov, Y.; Hickey, M. B. Celecoxib:Nicotinamide Dissociation: Using Excipients To Capture the Cocrystal's Potential. *Mol. Pharm.* **2007**, *4* (3), 386–400.
- (33) Etter, M. C.; Reutzel, S. M.; Choo, C. G. Self-Organization of Adenine and Thymine in the Solid State. *J. Am. Chem. Soc.* **1993**, *115* (10), 4411–4412.
- (34) Grzesiak, A. L.; Uribe, F. J.; Ockwig, N. W.; Yaghi, O. M.; Matzger, A. J. Polymer-Induced Heteronucleation for the Discovery of New Extended Solids. *Angew. Chemie - Int. Ed.* **2006**, *45* (16), 2553–2556.
- (35) Hasa, D.; Schneider Rauber, G.; Voinovich, D.; Jones, W. Cocrystal Formation through Mechanochemistry: From Neat and Liquid-Assisted Grinding to Polymer-Assisted Grinding. *Angew. Chemie* **2015**, *127* (25), 7479–7483.
- (36) Qiu, S.; Li, M. Effects of Cofomers on Phase Transformation and Release Profiles of Carbamazepine Cocrystals in Hydroxypropyl Methylcellulose Based Matrix Tablets. *Int. J. Pharm.* **2015**, *479* (1), 118–128.
- (37) Yazdani, M.; Briggs, K.; Jankovsky, C.; Hawi, A. The “high Solubility” definition of the Current FDA Guidance on Biopharmaceutical Classification System May Be Too Strict for Acidic Drugs. *Pharm. Res.* **2004**, *21* (2), 293–299.
- (38) Alshahateet, S. F. Synthesis and Supramolecularity of Hydrogen-Bonded Cocrystals of Pharmaceutical Model Rac-Ibuprofen with Pyridine Derivatives. *Mol. Cryst. Liq. Cryst.* **2010**, *533* (1), 152–161.
- (39) Aakeröy, C. B.; Beatty, A. M.; Helfrich, B. A. A High-Yielding Supramolecular Reaction. *J. Am. Chem. Soc.* **2002**, *124* (48), 14425–14432.
- (40) Aakeröy, C. B.; Beatty, A. M.; Helfrich, B. A.; Nieuwenhuyzen, M. Do Polymorphic Compounds Make Good Cocrystallizing Agents? A Structural Case Study That Demonstrates the Importance of Synthons Flexibility. *Cryst. Growth Des.* **2003**, *3* (2), 159–165.
- (41) Bathori, N. B.; Lemmerer, A.; Venter, G. A.; Bourne, S. A.; Cairns, M. R. Pharmaceutical Co-Crystals with Isonicotinamide-Vitamin B3, Clofibrilic Acid, and Diclofenac-and Two Isonicotinamide Hydrates. *Cryst. Growth Des.* **2011**, *11*, 75–87.
- (42) Thommes, M.; Ely, D. R.; Carvajal, M. T.; Pinal, R. Improvement of the Dissolution Rate of Poorly Soluble Drugs by Solid Crystal Suspensions. *Mol. Pharm.* **2011**, *8*, 727–735.
- (43) Padrela, L.; de Azevedo, E. G.; Velaga, S. P. Powder X-Ray Diffraction Method for the Quantification of Cocrystals in the Crystallization Mixture. *Drug Dev. Ind. Pharm.* **2012**, *38* (8), 923–929.
- (44) Guidelines, I. C. H. International Conference on Harmonization (ICH) Harmonized Tripartite Guideline, Note for Guidance on Validation of Analytical Procedures: Methodology. ICH Steering Committee 1996.
- (45) Leiserowitz, L. Molecular Packing Modes. Carboxylic Acids. *Acta Crystallogr. Sect. B Struct. Crystallogr. Cryst. Chem.* **1976**, *32*, 775–802.
- (46) Desiraju, G. R. *Crystal Engineering: The Design of Organic Solids*; Elsevier: Amsterdam, 1989.
- (47) Steiner, T. The Hydrogen Bond in the Solid State. *Angew. Chemie Int. Ed.* **2002**, *41* (1), 48–76.
- (48) Oswald, I. D. H.; Motherwell, W. D. S.; Parsons, S. A 1 : 2 Co-Crystal of Isonicotinamide and Propionic Acid. *Acta Crystallogr. Sect. E Struct. Reports Online* **2004**, *60* (12).

- (49) Vueba, M. L.; Pina, M. E.; Batista De Carvalho, L. A. E. Conformational Stability of Ibuprofen: Assessed by DFT Calculations and Optical Vibrational Spectroscopy. *J. Pharm. Sci.* **2008**, *97* (2), 845–859.
- (50) Silverstein, M.; Bassler, G. C.; Morrill, T. C. Spectrometric Identification of Organic Compounds ; J. Wiley & Son Inc.: New York, 1991; Vol. 5th, pp 117–123.
- (51) Logansen, A. V; Kurkchi, G. A.; Dement'eva, L. A. Infrared Spectra of Primary Amides in the ν NH Range. *J. Struct. Chem.* **1977**, *18* (4), 589–595.
- (52) Sharma, B. K. Infrared Spectroscopy. In *Spectroscopy*; GOEL Publishing House: Meerut Delhi, 2007; Vol. 20th, pp 309–311.
- (53) Filho, O. T.; Pinheiro, J. C.; da Costa, E. B.; Kondo, R. T.; de Souza, R. A.; Nogueira, V. M.; Mauro, A. E. Theoretical and Experimental Study of the Infrared Spectrum of Isonicotinamide. *J. Mol. Struct. THEOCHEM* **2006**, *763*, 175–179.
- (54) Socrates, G. *Infrared and Raman Characteristic Group Frequencies*; 2004.
- (55) Ramalingam, S.; Periandy, S.; Govindarajan, M.; Mohan, S. FT-IR and FT-Raman Vibrational Spectra and Molecular Structure Investigation of Nicotinamide: A Combined Experimental and Theoretical Study. *Spectrochim. Acta. A. Mol. Biomol. Spectrosc.* **2010**, *75* (5), 1552–1558.
- (56) Tothadi, S.; Desiraju, G. R. Unusual Co-Crystal of Isonicotinamide: The Structural Landscape in Crystal Engineering. *Philos. Trans. R. Soc. A Math. Phys. Eng. Sci.* **2012**, *370*, 2900–2915.
- (57) Steiner, T.; Desiraju, G. R. *The Weak Hydrogen Bond in Structural Chemistry and Biology*; Oxford University Press: New York, 1999.
- (58) Doherty, C.; York, P. Fresemide Crystal Forms; Solid State and Physicochemical Analyses. *Int. J. Pharm.* **1988**, *47* (1-3), 141–155.
- (59) Romero, A. J.; Savastano, L.; Rhodes, C. T. Monitoring Crystal Modifications in Systems Containing Ibuprofen. *Int. J. Pharm.* **1993**, *99* (2–3), 125–134.
- (60) Lu, E.; Rodriguez-Hornedo, N.; Suryanarayanan, R. A Rapid Thermal Method for Cocrystal Screening. *Cryst. Eng. Commun.* **2008**, *10*, 665–668.
- (61) Frišćić, T.; Jones, W. Benefits of Cocrystallisation in Pharmaceutical Materials Science: An Update. *J. Pharm. Pharmacol.* **2010**, *62*, 1547–1559.
- (62) Schultheiss, N.; Newman, A. W. Pharmaceutical Cocrystals and Their Physicochemical Properties. *Cryst. Growth Des.* **2009**, *9* (6), 2950–2967.
- (63) Almarsson, Ö.; Peterson, M. L.; Zaworotko, M. J. The A to Z of Pharmaceutical Cocrystals: A Decade of Fast Moving New Science and Patents. *Pharm. Pat. Anal.* **2012**, *1* (3), 313–327.
- (64) Alhalaweh, A.; Velaga, S. P. Formation of Cocrystals from Stoichiometric Solutions of Incongruently Saturating Systems by Spray Drying. *Cryst. Growth Des.* **2010**, *10* (8), 3302–3305.
- (65) Alhalaweh, A.; Kaialy, W.; Buckton, G.; Gill, H.; Nokhodchi, A.; Velaga, S. P. Theophylline Cocrystals Prepared by Spray Drying: Physicochemical Properties and Aerosolization Performance. *AAPS PharmSciTech* **2013**, *14* (1), 265–276.
- (66) Gryczke, A.; Schminke, S.; Maniruzzaman, M.; Beck, J.; Douroumis, D. Development and Evaluation of Orally Disintegrating Tablets (ODTs) Containing Ibuprofen Granules Prepared by Hot Melt Extrusion. *Colloids Surfaces B Biointerfaces* **2011**, *86* (2), 275–284.
- (67) Quentiros, D. A.; Allemandi, D. A.; Manzo, R. H. Equilibrium and Release Properties of Aqueous Dispersions of Non-Steroidal Anti-Inflammatory Drugs

- Complexed with Polyelectrolyte Eudragit E 100. *Sci. Pharm.* **2012**, *80* (2), 487–496.
- (68) Onoue, S.; Kojo, Y.; Aoki, Y.; Kawabata, Y.; Yamauchi, Y.; Yamada, S. Physical Chemical and Pharmacokinetic Characterization of Amorphous Solid Dispersion of Tranilast with Enhanced Solubility in Gastric Fluid and Improved Oral Bioavailability. *Drug Metab. Pharmacokinet. Adv. Publ.* **2012**.
- (69) Acton, Q. A. *Sugar Alcohols—Advances in Research and Application*; ScholarlyEditions: Atlanta, Georgia, 2013; Vol. 2013.
- (70) Aakeröy, C. B.; Grommet, A. B.; Desper, J. Co-Crystal Screening of Diclofenac. *Pharmaceutics* **2011**, *3* (3), 601–614.
- (71) Alatas, F.; Soewandhi, S. N.; Sasongko, L.; Ismunandar; Uekusa, H. Cocrystal Formation between Didanosine and Two Aromatic Acids. *Int. J. Pharm. Pharm. Sci.* **2013**, *5* (Suppl 3), 275–280.
- (72) Allen, L. V. J.; Yanchick, V. A.; Maness, D. D. Dissolution Rates of Corticosteroids Utilizing Sugar Glass Dispersions. *J. Pharm. Sci.* **1977**, *66* (4), 494–497.
- (73) Leuner, C.; Dressman, J. Improving Drug Solubility for Oral Delivery Using Solid Dispersions. *Eur. J. Pharm. Biopharm.* **2000**, *50* (1), 47–60.
- (74) Perissutti, B.; Newton, J. M.; Podcizek, F.; Rubessa, F. Preparation of Extruded Carbamazepine and PEG 4000 as a Potential Rapid Release Dosage Form. *Eur. J. Pharm. Biopharm.* **2002**, *53* (1), 125–132.
- (75) Li, C.; Li, C.; Le, Y.; Chen, J.-F. Formation of Bicalutamide Nanodispersion for Dissolution Rate Enhancement. *Int. J. Pharm.* **2011**, *404* (1–2), 257–263.
- (76) Eddleston, M. D.; Patel, B.; Day, G. M.; Jones, W. Cocrystallization by Freeze-Drying: Preparation of Novel Multicomponent Crystal Forms. *Cryst. Growth Des.* **2013**, *13* (10), 4599–4606.
- (77) Rumondor, A. C. F.; Stanford, L. A.; Taylor, L. S. Effects of Polymer Type and Storage Relative Humidity on the Kinetics of Felodipine Crystallization from Amorphous Solid Dispersions. *Pharm. Res.* **2009**, *26* (12), 2599–2606.
- (78) Stevens, M. J.; Covas, J. A. *Extruder Principles and Operation*; Chapman & Hall: 2-6 Boundary Row, London SE1 8HN, UK, 1995; Vol. Second edi.
- (79) Dreiblatt, A. Process Design. In *Pharmaceutica Extrusion Technology*; Ghebre-Sellassie, I., Martin, C., Eds.; Marcel Dekker, Inc.: New York, 2003; pp 153–169.
- (80) Thiele, W. Twin-Screw Extrusion and Screw Design. In *Pharmaceutical Extrusion Technology*; Ghebre-Sellassie, I., Martin, C., Eds.; Marcel Dekker, Inc: New York, 2003; pp 69–98.
- (81) Douroumis, D. *Hot-Melt Extrusion: Pharmaceutical Extrusions*; John Wiley & Sons Ltd: West Sussex, UK, 2012.
- (82) Reitz, E.; Podhaisky, H.; Ely, D.; Thommes, M. Residence Time Modeling of Hot Melt Extrusion Processes. *Eur. J. Pharm. Biopharm.* **2013**, *85* (3 PART B), 1200–1205.

